



ELSEVIER

doi:10.1016/j.gca.2005.04.012

## Molecular biogeochemistry of sulfate reduction, methanogenesis and the anaerobic oxidation of methane at Gulf of Mexico cold seeps

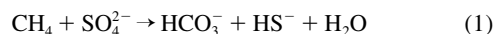
BETH! ORCUTT,<sup>1</sup> ANTJE BOETIUS,<sup>2,3</sup> MARCUS ELVERT,<sup>4</sup> VLADIMIR SAMARKIN,<sup>1</sup> and SAMANTHA B. JOYE<sup>1,\*</sup><sup>1</sup>Department of Marine Sciences, University of Georgia, Athens, GA 30602, USA<sup>2</sup>Max Planck Institute for Marine Microbiology, Celsiusstrasse 1, 28359 Bremen, Germany<sup>3</sup>International University Bremen, 28725 Bremen, Germany<sup>4</sup>Research Center Ocean Margins, Department of Organic Geochemistry, University of Bremen, 28359 Bremen, Germany

(Received November 29, 2004; accepted in revised form April 26, 2005)

**Abstract**—The anaerobic oxidation of methane in aquatic environments is a globally significant sink for a potent greenhouse gas. Significant gaps remain in our understanding of the anaerobic oxidation of methane because data describing the distribution and abundance of putative anaerobic methanotrophs in relation to rates and patterns of anaerobic oxidation of methane activity are rare. An integrated biogeochemical, molecular ecological and organic geochemical approach was used to elucidate interactions between the anaerobic oxidation of methane, methanogenesis, and sulfate reduction in sediments from two cold seep habitats (one brine site, the other a gas hydrate site) along the continental slope in the Northern Gulf of Mexico. The results indicate decoupling of sulfate reduction from anaerobic oxidation of methane and the contemporaneous occurrence of methane production and consumption at both sites. Phylogenetic and organic geochemical evidence indicate that microbial groups previously suggested to be involved in anaerobic oxidation of methane coupled to sulfate reduction were present and active. The distribution and isotopic composition of lipid biomarkers correlated with microbial distributions, although concrete assignment of microbial function based on biomarker profiles was complicated given the observed overlap of competing microbial processes. Contemporaneous activity of anaerobic oxidation of methane and bicarbonate-based methanogenesis, the distribution of methane-oxidizing microorganisms, and lipid biomarker data suggest that the same microorganisms may be involved in both processes. Copyright © 2005 Elsevier Ltd

### 1. INTRODUCTION

A substantial increase in atmospheric methane concentration over the past two centuries has contributed to present-day global warming (Intergovernmental Panel on Climate Change, 2000). Additional evidence links atmospheric methane concentrations with global-scale climate change throughout geologic time (Katz et al., 1999; Hesselbo et al., 2000; Thomas et al., 2002). Though the largest known reservoirs of methane occur in marine sediments as methane hydrate (Kvenvolden, 1988), the contribution of this reservoir to the atmospheric methane pool is moderated by the anaerobic oxidation of methane (AOM). Rate measurements, geochemical profiles and reaction-transport modeling results indicate methane is consumed anaerobically using sulfate as electron acceptor according to the following net equation (Barnes and Goldberg, 1976; Reeburgh, 1976; Devol et al., 1984; Iversen and Jørgensen, 1985; Hoehler et al., 1994):



Although the correlation between AOM and sulfate reduction (SR) has been observed in a variety of environments, the biogeochemical mechanism behind AOM remains to be determined (Hoehler et al., 1994; Valentine and Reeburgh, 2000; Sørensen et al., 2001; Nauhaus et al., 2002). Phylogenetic and organic geochemical data have identified a putative syntrophic consortia of anaerobic methanotrophs and sulfate reducing bac-

teria that mediate AOM, but the metabolic intermediate(s) exchanged between the participating microbes is unknown (Hoehler et al., 1994; Elvert et al., 1999; Boetius et al., 2000; Hinrichs et al., 2000; Orphan et al., 2001b). The anaerobic methanotrophs (named ANME) are phylogenetically related to methanogenic archaea, while the sulfate reducing bacteria are associated with the *Desulfosarcinal/Desulfococcus* cluster (Boetius et al., 2000; Orphan et al., 2001a; Knittel et al., 2003). Additional molecular data suggest the involvement of multiple archaeal and bacterial groups in AOM (Hinrichs et al., 2000; Pancost et al., 2000; Orphan et al., 2001a; Thomsen et al., 2001; Orphan et al., 2002; Teske et al., 2002). Available 16S clone library evidence suggests that classical methanogens are rare in ANME communities, with the exception of the hydrothermally-heated sediments of the Guaymas Basin (Teske et al., 2002). Recent genomic and proteomic data from samples naturally enriched in ANME microorganisms showed that they contained modified methanogenic genes and enzymes, suggesting that the biochemical mechanism of AOM is a reversal of the bicarbonate-based methanogenesis (Bi-MOG) pathway (Hallam et al., 2003, 2004; Krüger et al., 2003). The question remains as to whether ANME microorganisms switch between AOM and methanogenesis (MOG) as a function of environmental conditions.

The processes of AOM, MOG and SR may interact in a variety of ways but no previous work has documented patterns of these processes in comparison to microbiological and geochemical variables. While a number of studies of surficial sediments have focused on interactions between SR and AOM (Hoehler et al., 1994; Hansen et al., 1998; Joye et al., 2004) or

\* Author to whom correspondence should be addressed (mjoye@uga.edu).

SR and MOG (Oremland and Polcin, 1982; Lovley and Klug, 1986), few have investigated potential interaction(s) between AOM and MOG. Available data show that rates of MOG vary considerably in comparison to AOM rates. In sediments from a barrier lagoon (Cape Lookout Bight, USA), AOM occurred in sulfate-depleted sediments at ~10% the rate of Bi-MOG; both AOM and Bi-MOG were stimulated when sediments were amended with sulfate (Hoehler et al., 1994). In contrast, in sediments from another coastal environment (Eckernförde Bay, Germany), AOM was limited to sulfate-containing sediments, and Bi-MOG rates were ~40% to 50% of AOM rates (Treude et al., 2005). In benthic microbial mats from the Black Sea, Bi-MOG rates were comparable to AOM and SR rates (Treude, 2003); the majority of archaeal biomass in these mats was associated with ANME-1 and ANME-2 (based on 16S clone libraries and FISH; Knittel et al., 2005). Thus, the activity of AOM and MOG exhibit variability with respect to the geochemical environment, being restricted to sulfate-depleted sediments in one case and sulfate-replete sediments in another, and the relative magnitude of rates of MOG to those of AOM spanned a considerable range, from 10% to 100% of AOM rates. The observed variation in patterns of methanotrophic and methanogenic activities could result from variability in geochemical factors, microbial community structure, or additional, unknown factors.

To further understand why the processes of AOM and SR appear to be tightly coupled in some cases (Hinrichs and Boetius, 2002) but only loosely coupled in others (Joye et al., 2004), and to document the interaction between AOM and MOG, we investigated these processes in two types of cold seep habitats on the continental slope in the Northern Gulf of Mexico. One site featured a brine pool, the absence of surficial gas hydrates, and a fluid flux of methane-saturated brine; the second site was characterized by surficial and deep gas hydrates and contemporaneous seepage of methane, other alkanes and oil. We used an integrated biogeochemical, molecular biologic and organic geochemical approach to holistically characterize the environment.  $^{14}\text{C}$ - and  $^{35}\text{S}$ -based radiotracer assays revealed weak coupling between AOM and SR (e.g., <1:1 stoichiometry as would be expected from Eqn. 1) and contemporaneous activity of AOM and Bi-MOG, with Bi-MOG rates amounting to ~10% of AOM rates. Microbial distribution and lipid biomarker data illustrated the abundance of putative methanotrophic Archaea, but these data were insufficient to determine concretely the metabolic role of these microbes since AOM and MOG activity overlapped.

## 2. METHODS

### 2.1. Study Sites and Sample Collection

Along the continental slope in the northern Gulf of Mexico, salt tectonics generate fault networks that act as natural migration pathways for oil, gas, and brine fluid from deep reservoirs to surficial sediments (Behrens, 1988; Kennicutt et al., 1988; Aharon, 1994). When pressure and temperature conditions on the bottom are suitable, high gas fluxes result in gas hydrate formation (Sloan, 1990; Kvenvolden, 1993; Milkov and Sassen, 2000; Dickens, 2001). Seepage of gas charged brine vs. oil and gas support distinct cold seep environments dominated by brine pools and mud volcanoes (in the former case) or gas hydrates (in the latter case). Both types of cold seeps are characterized by abundant chemosynthetically-based communities of free-living bacteria (e.g., *Beggiatoa*, *Thioploca*, *Thiomargarita*) and symbiotic macro-

fauna (e.g., *Lamellibranchia* sp. and *Escarpia* sp. tube worms with thiotrophic symbionts, and *Bathymodiolus*-like mussels with methanotrophic symbionts (MacDonald et al., 1989, 1994, 2003; Sassen and MacDonald, 1994; Sassen et al., 2001).

Samples were collected during dives of the manned submersible *Johnson Sea Link II* operated from the *R/V Seward Johnson II* (Harbor Branch Oceanographic Institute) during the summer of 2002 using methods described previously (Joye et al., 2004). One suite of samples was collected at a brine-influenced seep (GC233; 27:43.3844N, 91:16.6054W, 650 m water depth). Seepage was dominated by gas-charged brine; no gas hydrate or oil seepage was evident (MacDonald et al., 1990a; Sassen et al., 1994). At this site, a brine pool (~190 m<sup>2</sup>; MacDonald et al., 1990b) was surrounded by concentric rings (3–7 m wide) of densely-packed mussels (MacDonald et al., 2003). Sediment cores were collected along the outer edge of the mussel bed, ~3 to 5 m from the edge of the brine pool, where microbial mats dominated by a *Thiomargarita namibiensis*-relative (Kalenetra et al., 2005) were abundant. The second suite of samples was collected from a hydrocarbon-influenced seep in lease block GC232 (27:44.4566N, 91:18.9812W, 504 m water depth). The GC232 site lies ~4 km west of GC233 (De Beukelaer et al., 2003; Sager et al., 2003) and was characterized by abundant, large (~2 m in diameter) surficial gas hydrate mounds and seepage of methane and oil. The sediment surface was covered by a plush mat of vacuolate sulfide-oxidizing bacteria (*Beggiatoa* spp.). Sediment push cores (7 cm I.D., ~30 cm core tube length, average recovery of ~15 cm of sediment) were collected carefully using the robotic arm of the submersible. Upon return to the surface, cores were transferred immediately to an environmental lab held at bottom water temperature (~8°C) where all subsequent processing was conducted.

### 2.2. Core Sectioning, Porewater Collection and Analysis

Several replicate cores were recovered from an area of ~1 m<sup>2</sup>. One replicate core was used for each of the following procedures: (1) porewater and solid phase analyses, (2) AOM and SR rates, molecular ecology and lipid biomarkers samples, and (3) MOG rates. For porewater and solid phase sample collection, each core tube was fitted with a piston (black rubber stopper) and mounted on a hydraulic extruder. The sediment was extruded at 2-cm intervals into an Argon-filled glove bag in a cold room. At each depth interval, a 2-mL subsample was collected into a cut-off syringe for dissolved methane quantification. The sediment was transferred immediately to a 6-mL helium-purged serum vial that contained 2 mL of helium-purged 2 mol/L NaOH, which served to arrest biologic activity in the sample, and crimp sealed with a butyl rubber stopper. Another 1-mL subsample was collected into preweighed and precombusted glass vial for determination of porosity (determined by the change in weight after drying at 80°C to a constant weight). The remaining material was transferred into a PVC cup for attachment to a Reeburgh-type squeezer for porewater extraction (Joye et al., 2004). Sample fixation and analyses for quantifying dissolved methane (CH<sub>4</sub>), sulfide (HS<sup>-</sup>), sulfate (SO<sub>4</sub>), chloride (Cl<sup>-</sup>) and bicarbonate (DIC or HCO<sub>3</sub><sup>-</sup>) followed the methods of Joye et al. (2004). Samples for volatile fatty acids analysis, primarily for acetate (CH<sub>3</sub>COO<sup>-</sup>), were filtered (0.2 μm) and stored frozen until quantification using HPLC (Albert and Martens, 1997).

### 2.3. Rate Measurements

To determine AOM and SR rates, one to six subcores (30 cm long × 2.54 cm i.d.) were collected from a core (7 cm i.d.) by manual insertion. Each Plexiglas subcore had predrilled, silicone-sealed injection ports at 1 cm intervals along one side of the core. The water phase overlying the core was maintained during subcoring and the ends of the core tubes were sealed securely with black rubber stoppers. For AOM, 100 μL of dissolved  $^{14}\text{C}$  tracer (~35,000 dpm in slightly alkaline milliQ water) was injected into each silicone-filled port. Cores were incubated for 12 h at bottom water temperature (8°C). Following incubation, cores were extruded and subsamples were collected at 1 cm intervals and immediately transferred to 20-mL glass vials containing 2 mL of 2 mol/L NaOH (which served to arrest biologic activity and fix  $^{14}\text{C}$ -CO<sub>2</sub> and  $^{14}\text{C}$ -HCO<sub>3</sub><sup>-</sup>). Each vial was sealed with a Teflon-lined screw cap, vortexed to mix the sample and base, and immediately frozen. Time

zero samples were fixed immediately after tracer injection. The specific activity of the tracer ( $^{14}\text{CH}_4$ ) was determined by injecting 100  $\mu\text{L}$  directly into scintillation cocktail (Scintiverse BD) followed by liquid scintillation counting (Joye et al., 1999). The accumulation of  $^{14}\text{C}$  product ( $^{14}\text{CO}_2$ ) was determined by acid digestion following the method of Joye et al. (1999, 2004). The AOM rate was calculated using Eqn. 2:

$$\text{AOM rate} = [\text{CH}_4] \times \alpha_{\text{CH}_4} / t \times (a^{-14}\text{CO}_2 / a^{-14}\text{CH}_4) \quad (2)$$

Here, the AOM rate is expressed as  $\text{nmol CH}_4$  oxidized per  $\text{cm}^3$  sediment per day ( $\text{nmol cm}^{-3} \text{d}^{-1}$ ),  $[\text{CH}_4]$  is the methane concentration ( $\text{nmol/L}$ ),  $\alpha_{\text{CH}_4}$  is the isotope fractionation factor for AOM (1.06; Alperin and Reeburgh, 1988),  $t$  is the incubation time (d),  $a^{-14}\text{CO}_2$  is the activity of the product pool, and  $a^{-14}\text{CH}_4$  is the activity of the substrate pool.

For SR rate measurements, each port was injected with 100  $\mu\text{L}$  of slightly alkaline milliQ water containing  $\sim 2 \mu\text{Ci}$  of  $\text{Na}_2^{35}\text{SO}_4$ . Cores were incubated and sectioned as described above. Each section was transferred to a 50-mL centrifuge tube containing 10 mL of 20% zinc acetate to halt microbial activity and fix  $\text{H}_2^{35}\text{S}$  as  $\text{Zn}^{35}\text{S}$ . The accumulation of  $\text{H}_2^{35}\text{S}$  product was recovered in a one-step hot chromous acid digestion (Canfield et al., 1986; Fossing and Jørgensen, 1989). The activity of  $\text{ZnS}$  and sulfate fractions was determined by scintillation counting. The sulfate reduction rate was calculated using Eqn. 3:

$$\text{SR rate} = [\text{SO}_4] \times \alpha_{\text{SO}_4} / t \times (a - \text{H}_2^{35}\text{S} / a^{-35}\text{SO}_4) \quad (3)$$

The SR rate is expressed as  $\text{nmol SO}_4$  reduced  $\text{cm}^{-3} \text{d}^{-1}$ ,  $\alpha_{\text{SO}_4}$  is the isotope fractionation factor for sulfate reduction (1.06; Jørgensen, 1978),  $[\text{SO}_4]$  is the pore water sulfate concentration ( $\text{mmol/L}$ ),  $t$  is incubation time (d),  $a - \text{H}_2^{35}\text{S}$  is the activity of the product pool, and  $a^{-35}\text{SO}_4$  is the activity of the substrate pool.

Rates of Bi-MOG and acetoclastic methanogenesis (Ac-MOG) were determined by incubating samples in gas-tight, closed-tube vessels without headspace, to prevent the loss of gaseous  $^{14}\text{CH}_4$  product during sample manipulation. For collection of subsamples, a polycarbonate manifold containing 8 predrilled holes that were slightly larger than the diameter of the sample tubes was placed on top of the sediment core. The sediment was extruded into the manifold at 2 cm intervals and then a stainless steel blade was inserted at the base of the device to isolate the section from the remaining sediment. Next, 6–8 glass tubes (20-mL Pyrex Hungate culture tubes with the rounded end removed) were inserted through the predrilled holes into the sediment, stopping at the blade. Tubes were sealed using custom-designed plungers (black Hungate stoppers with the lip removed containing a plastic “tail” that was run through the stopper) were inserted at the base of the tube; the sediment was then pushed via the plunger to the top of the tube until a small amount protruded through the tube opening. A butyl rubber septa was then eased into the tube opening to displace sediment in contact with the atmosphere and close the tube, which was then sealed with an open-top screw cap. The rubber materials used in these assays were boiled in 1 N NaOH for 1 h, followed by several rinses in boiling milliQ, to leach potentially toxic substances.

A volume of radiotracer solution (100  $\mu\text{L}$  of  $^{14}\text{C-HCO}_3^-$  tracer [ $\sim 1 \times 10^7$  dpm in slightly alkaline milliQ water] or  $1,2-^{14}\text{C-CH}_3\text{COO}^-$  tracer [ $\sim 5 \times 10^6$  dpm in slightly alkaline milliQ water]) was injected into each sample. Samples were incubated as described above and then 2 mL of 2 N NaOH was injected through the top stopper into each sample to terminate biologic activity (time zero samples were fixed before tracer injection). Samples were mixed to evenly distribute NaOH through the sample. Production of  $^{14}\text{CH}_4$  was quantified by stripping methane from the tubes with an air carrier, converting the  $^{14}\text{CH}_4$  to  $^{14}\text{CO}_2$  in a combustion furnace, and subsequent trapping of the  $^{14}\text{CO}_2$  in NaOH as carbonate (Crill and Martens, 1986; Cragg et al., 1990). Activity of  $^{14}\text{CO}_2$  was measured subsequently by liquid scintillation counting. The rates of Bi-MOG and Ac-MOG rates were calculated using Eqn. 4 and 5, respectively:

$$\text{Bi-MOG rate} = [\text{HCO}_3^-] \times \alpha_{\text{HCO}_3^-} / t \times (a^{-14}\text{CH}_4 / a^{-14}\text{CO}_3^-) \quad (4)$$

$$\text{Ac-MOG rate} = [\text{CH}_3\text{COO}^-] \times \alpha_{\text{CH}_3\text{COO}^-} / t \times (a^{-14}\text{CH}_4 / a^{-14}\text{CH}_3\text{COO}^-) \quad (5)$$

Both rates are expressed as  $\text{nmol HCO}_3^-$  or  $\text{CH}_3\text{COO}^-$ , respectively, reduced  $\text{cm}^{-3} \text{d}^{-1}$ ,  $\alpha_{\text{HCO}_3^-}$  and  $\alpha_{\text{CH}_3\text{COO}^-}$  are the isotope fractionation factors for MOG (assumed to be 1.06; Krzycki et al., 1987; Gelwick et al., 1994).  $[\text{HCO}_3^-]$  and  $[\text{CH}_3\text{COO}^-]$  are the pore water bicarbonate ( $\text{mmol/L}$ ) and acetate ( $\mu\text{mol/L}$ ) concentrations, respectively,  $t$  is incubation time (d),  $a^{-14}\text{CH}_4$  is the activity of the product pool, and  $a^{-14}\text{CO}_3^-$  and  $a^{-14}\text{CH}_3\text{COO}^-$  are the activities of the substrate pools. All rates reflect correction for porosity where appropriate.

## 2.4. Microbial Distribution

The abundance and associations of specific microbial groups were evaluated using fluorescence in situ hybridization (FISH) techniques that targeted 16S rRNA (Pernthaler et al., 2002). Due to high background fluorescence from oil in sediment preparations, mono-labeled fluorescent oligonucleotide probes were not sensitive enough for robust detection of microbes; thus, an immunochemical-based FISH protocol was used to increase signal intensity (Pernthaler and Amann, 2004). In catalyzed reporter deposition FISH (CARD-FISH; also described elsewhere as the tyramide signal amplification [TSA] system; Schönhuber et al., 1997), multiple copies of fluorescently-labeled tyramide molecules bind to oligonucleotide probes bound with horseradish peroxidase (HRP), which increases the fluorescent label per copy of rRNA in the target cells relative to mono-labeled FISH.

Sediment samples for cell counts and FISH were fixed in 3.7% formaldehyde buffered in 1 $\times$ PBS (140  $\text{mmol/L}$  NaCl, 10  $\text{mmol/L}$  sodium phosphate, pH 7.6) for 4 to 8 h at 4°C, washed in 1 $\times$ PBS, and subsequently stored in 1:1 1 $\times$ PBS:ethanol (EtOH) at  $-20^\circ\text{C}$  until analysis (Boetius et al., 2000). Immobilization of cells on filters for hybridization followed methods described previously (Boetius et al., 2000). Total cell abundance of single cells and cells in aggregates (estimated by dividing aggregate size by average size of spherical cells in aggregate) was determined using acridine orange direct counting (Orcutt et al., 2004).

The application of FISH probes and amplification of the fluorescence signal followed the methods of Pernthaler et al. (2002), as modified for sediment applications. Hybridization filters were covered in a thin layer of 0.1% (wt/vol) low-melting point agarose (MetaPhor, Bioproducts, Rockland, Maine), dried at 46°C for 1 h, dehydrated with 80% EtOH and dried at room temperature (RT). Endogenous peroxidases in fixed cells were inactivated by incubating filters in 0.01  $\text{mol/L}$  HCl for 10 min at RT. Permeabilization of microbial cell walls was required to permit passage of the large HRP-labeled rRNA probes into the cells; these procedures did not compromise the integrity of the cell structure. Filters were briefly washed in 1 $\times$ PBS, incubated in SDS solution (0.5% [wt/vol] sodium dodecyl sulfate in 1 $\times$ PBS) for 8 min at RT, washed again in 1 $\times$ PBS, incubated in fresh lysozyme solution (0.05  $\text{mol/L}$  EDTA, 0.1  $\text{mol/L}$  Tris [pH 8], 10  $\text{mg mL}^{-1}$  lysozyme) for 1 h at 37°C, serially washed in 1 $\times$ PBS, MilliQ water, and 80% EtOH and then dried at RT. This permeabilization strategy resulted in robust enumeration of sediment *Archaea* and *Bacteria* with minimal increase in background fluorescence, loss of target cells, or unspecific binding of rRNA probes (data not shown).

Hybridization protocols were performed as described previously (Pernthaler et al., 2002). Filter sections were incubated in appropriate hybridization buffers (900  $\text{mmol/L}$  NaCl, 20  $\text{mmol/L}$  Tris-HCl, varying concentrations of formamide [FA; 99.9% molecular biology grade, see below for percentage used], 1% blocking reagent [Roche, Basel, Switzerland], 10% [wt/vol] dextran sulfate) with HRP-labeled probes (Thermo Biosciences GmbH, Germany;  $\sim 27 \text{ pmol mL}^{-1}$  final concentration) at 35°C for 2 h with gentle mixing. Probes and corresponding FA concentrations in hybridization buffers used were as follows: EUB338 I-III (Daims et al., 1999) for *Bacteria* (55% FA), ARCH915 (Amann et al., 1990) for *Archaea* (55% FA), ANME1-350 (Boetius et al., 2000) for the ANME1 clade of *Euryarchaeota* (40% FA), E-IMSX932 (Boetius et al., 2000) for the ANME2 clade of *Euryarchaeota* (40% FA), DSS658 (Manz et al., 1998) for the *Desulfosarcina* spp./*Desulfococcus* spp./*Desulfofrigus* spp./*Desulfobaba* spp. clades of sulfate reducing  $\delta$ -Proteobacteria (55% FA), and NON338 (Wallner et al., 1993) as a non-sense negative control probe to check for unspecific binding (55% FA). Background signal from the nonsense probe NON338 was negligible, and thus, is not reported. Probe specificity was verified by hybridization in samples of defined microbial compo-

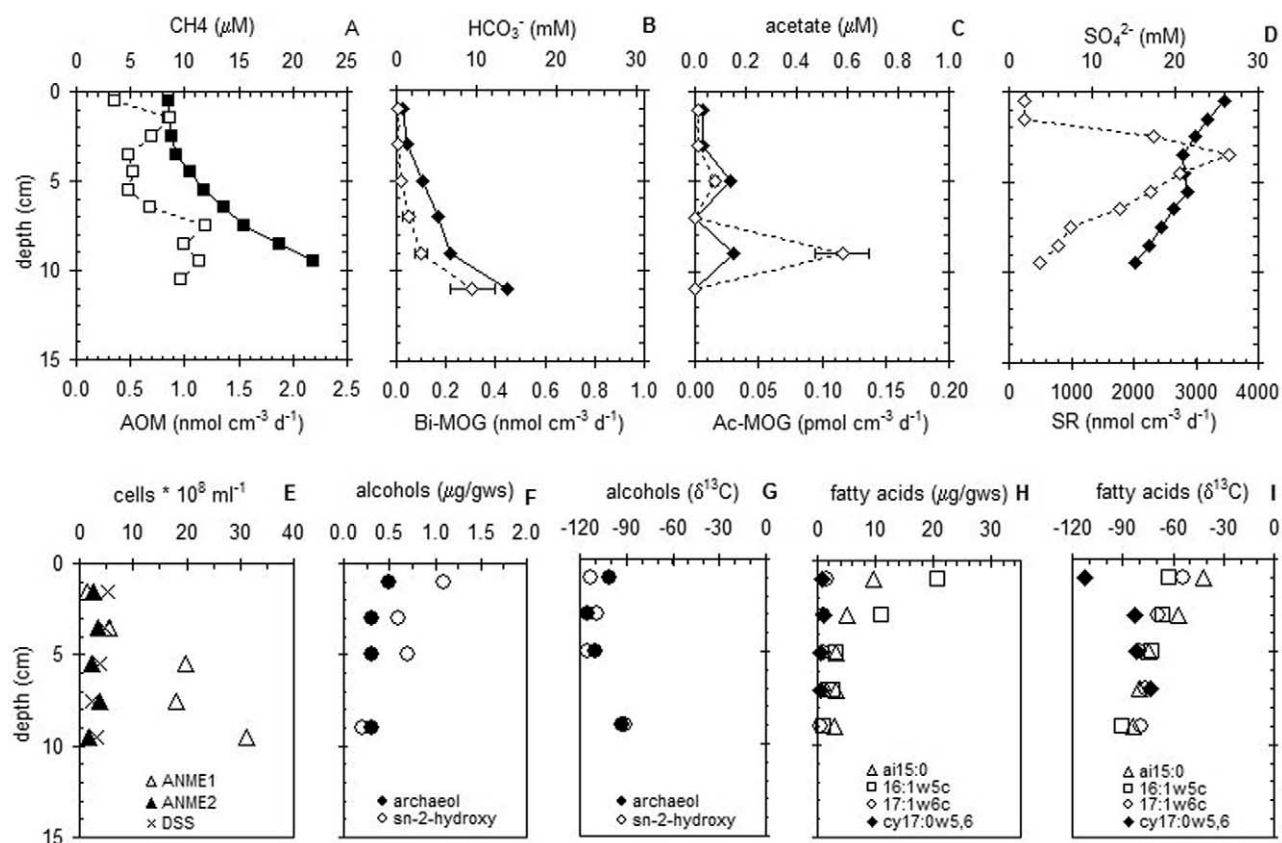


Fig. 1. Composite profiles of geochemistry, rates of microbial processes, microorganism diversity and abundance, and abundance and isotopic composition of select lipid biomarkers in sediments collected from underneath a bacterial mat at a brine pool cold seep (GC233) in the Gulf of Mexico. In (A) to (D), filled symbols represent the concentration while open symbols represent the rate. In (F) to (I), abbreviated names of lipids are presented in legends; see text for explanation of abbreviations. (A) Methane ( $\text{CH}_4$ ) concentration and AOM rate; (B) dissolved inorganic carbon ( $\text{HCO}_3^-$ ) concentration and the rate of autotrophic methanogenesis (Bi-MOG); (C) acetate concentration and the rate of acetoclastic methanogenesis (Ac-MOG); (D) sulfate ( $\text{SO}_4^{2-}$ ) concentration and SR rate; (E) total abundance of specific groups of microorganisms as determined by CARD-FISH; (F) abundance of select archaeal lipid biomarkers extracted from sediment; (G)  $\delta^{13}\text{C}$  isotopic composition of same select archaeal lipid biomarkers; (H) abundance of select bacterial lipid biomarkers extracted from sediment; (I)  $\delta^{13}\text{C}$  isotopic composition of same select bacterial lipid biomarkers. All panels scaled to the same depth axis (given in [A] and [E] in cm below seafloor).

sition. Synthesis of fluorescently-labeled (Cy3, carboxyfluorescein, Alexa<sub>546</sub> and Alexa<sub>488</sub> dyes) tyramides followed the method of Hopman et al. (1998); application of tyramide to hybridized samples followed the method of Pernthaler et al. (2002). To simultaneously visualize multiple microbial groups, hybridization and fluorescence labeling was carried out in sequence using probes labeled with different fluorescent dyes. Each probe was applied, hybridized, and then signal amplified. Then, the HRP-label was inactivated by incubating in 0.01 mol/L HCl for 10 min at RT followed by a 1×PBS wash. The next hybridization was performed in a similar manner.

Hybridized filters were covered with 4',6'-diamidino-2-phenylindole (DAPI)-amended mounting solution (1 part 1×PBS, 5.5 parts Citifluor mountant, 1 part Vecta Shield mountant, 2  $\mu\text{g ml}^{-1}$  DAPI) for total cell enumeration. Cell counts using DAPI was comparable to measurements using AODC (data not shown). Roughly 40 fields (1000–1600 DAPI cells) were examined for each sample/probe combination to determine average cell counts. Percentages of each microbial group were determined by the representative proportion of hybridized cells to DAPI cells per field. Samples were visualized under 1000× oil-immersion magnification using an Axioplan II Zeiss epifluorescence microscope equipped with an HBO 100-W Hg vapor lamp, with appropriate filters sets for Cy3 and Alexa<sub>546</sub> (Chroma, Brattleborough, Conn.), carboxyfluorescein and Alexa<sub>488</sub> (Zeiss09; Zeiss, Germany), and DAPI (Zeiss01; Zeiss, Germany) fluorescence.

## 2.5. Lipid Biomarkers

Lipid biomarkers were extracted from ~1.4 g wet sediment and analyzed according to previously described methods (Boetius et al., 2000; Elvert et al., 2001, 2003). Briefly, total lipids were extracted following ultrasonication in methanol/dichloromethane. The total lipid extract (TLE) was saponified with 6% KOH in methanol; neutral lipids were removed from the saponified TLE by extraction with *n*-hexane. Fatty acids were obtained from the remaining TLE phase by acidification to pH 1 and subsequent extraction with *n*-hexane. Carboxylic (fatty) acid methyl esters (FAMES) were generated from the fatty acids by reaction with 14%  $\text{BF}_3$  in methanol and subsequent re-extraction with *n*-hexane. Alcohol lipid fractions were obtained from the neutral lipid extract using liquid chromatography separation on a column of activated silica suspended in dichloromethane. Alcohol derivatives were generated by reaction with pyridine and BSTFA. Lipid biomarkers were identified by coupled gas chromatography-mass spectrometry (GC-MS) using a Thermoquest Trace GC interfaced to a Finnigan Trace MS. Compounds were identified by comparison with mass spectra from known compounds. Carbon isotopic compositions of individual biomarkers were determined by coupled gas chromatography-isotope ratio mass spectrometry (GC-IRMS) using HP 6890 Series GC interfaced via a Finnigan Combustion Interface III to a Finnigan Delta plus mass spectrometer. The reported biomarker  $\delta^{13}\text{C}$  values

Table 1. Concentrations of sulfide ( $\text{H}_2\text{S}$ ) and chloride ( $\text{Cl}^-$ ), total cell abundance, and percentage of cells (as determined by CARD-FISH) that were *Bacteria* (EUB), *Archaea* (ARC), of the ANME-1 clade of *Euryarchaeota* (ANME1), of the ANME-2 clade of *Euryarchaeota* (ANME2), or of the *Desulfosarcina/Desulfococcus* spp. clades of  $\delta$ -proteobacteria (DSS) in sediments from the Gulf of Mexico.

Site + dive	Depth (cmbsf)	$\text{H}_2\text{S}$ (mmol/L)	$\text{Cl}^-$ (mmol/L)	Cells ( $10^9 \text{ mL}^{-1}$ )	EUB (% cells)	ARC (% cells)	ANME1 (% cells)	ANME2 (% cells)	DSS (% cells)
GC233 (brine pool)	1	0.2	544.9	5.4	64.5	5.6	2.7	4.6	10.0
	3	1.0	531.4	4.8	55.3	16.9	11.8	7.4	9.9
	5	2.9	571.1	5.5	28.9	41	36.1	4.4	7.0
Dive 4458	7	4.6	—	5.4	22.8	37.6	33.4	6.9	4.4
	9	—	509.5	6.8	11.7	48.3	45.9	2.4	4.6
	11	7.0	—	—	—	—	—	—	—
	11	7.0	—	—	—	—	—	—	—
GC232 (hydrate)	1	11.9	556.7	3.7	78.5	4.4	2.5	0.0	18.8
	3	18.9	544.4	2.5	79.5	4.1	1.0	0.1	16.9
Dive 4459	5	20.1	535.3	2.2	79	12	3.7	1.0	12.2
	7	17.4	421.9	2.2	74	24.5	19.1	3.0	25.9
	9	17.8	468.6	—	—	—	—	—	—
	11	14.5	511.0	—	—	—	—	—	—

Dashes indicate no data.

have an analytical error of  $\pm 1.0\%$  and have been corrected for the introduction of additional carbon atoms during derivitization.

### 3. RESULTS

#### 3.1. Methane Turnover and Sulfate Reduction

In sediments collected from a microbial mat at the edge of the brine pool (GC233; MacDonald et al., 2003), methane

concentrations were well below saturation ( $<30 \mu\text{mol/L}$ ; Fig. 1A) and AOM rates were very low ( $<2 \text{ nmol cm}^{-3} \text{ d}^{-1}$ ; Fig. 1A), despite high turnover rates for  $^{14}\text{C}$ -methane ( $\sim 10\%$  turnover in 12 h). Dissolved inorganic carbon ( $\text{HCO}_3^-$ ) concentration increased steadily with depth, reaching a maximum of 14 mmol/L between 10 and 12 cm (Fig. 1B). Rates of Bi-MOG increased with depth but were low ( $<0.4 \text{ nmol cm}^{-3} \text{ d}^{-1}$ ; Fig.

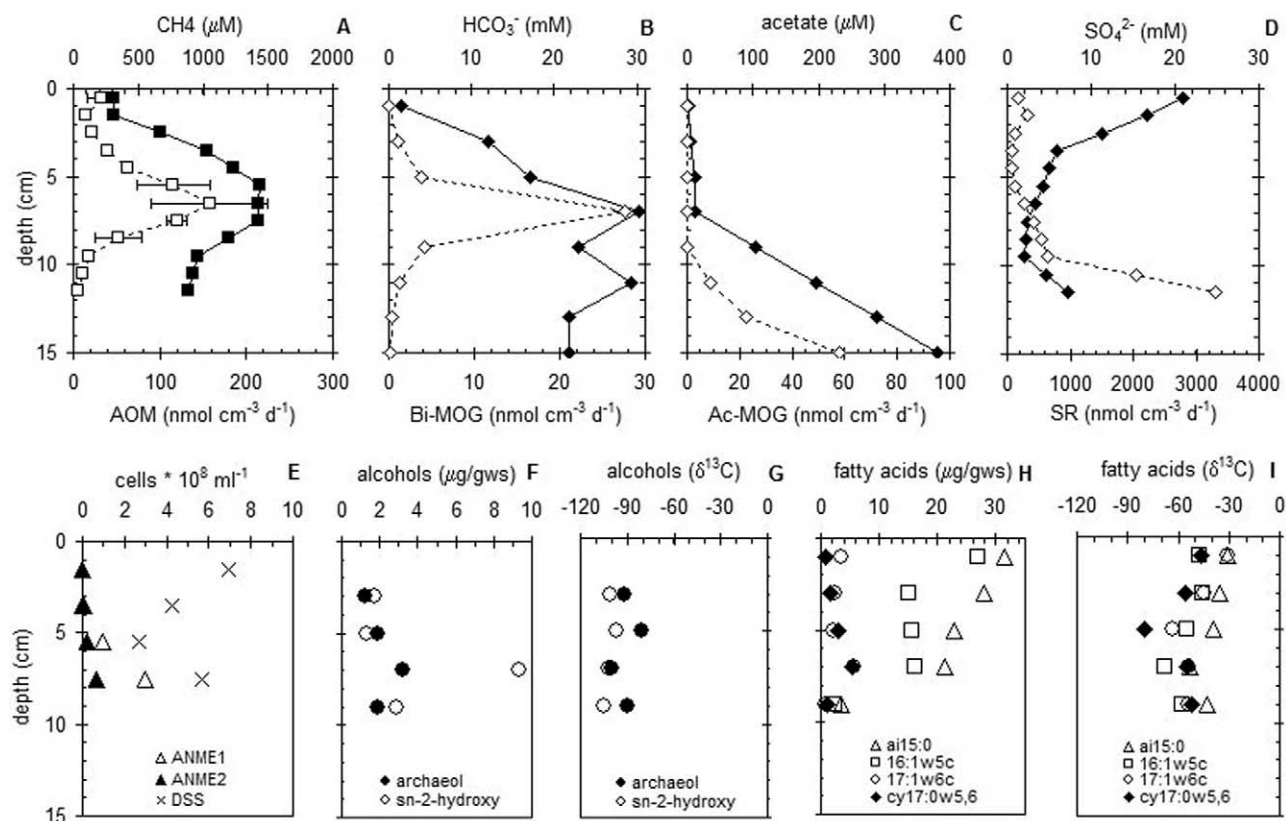


Fig. 2. Composite profiles of geochemistry, rates of microbial processes, microorganism diversity and abundance, and abundance and isotopic composition of select lipid biomarkers in sediments collected from underneath a bacterial mat at a gas hydrate cold seep (GC232) in the Gulf of Mexico. Panels and symbols identical to those presented in Figure 1.

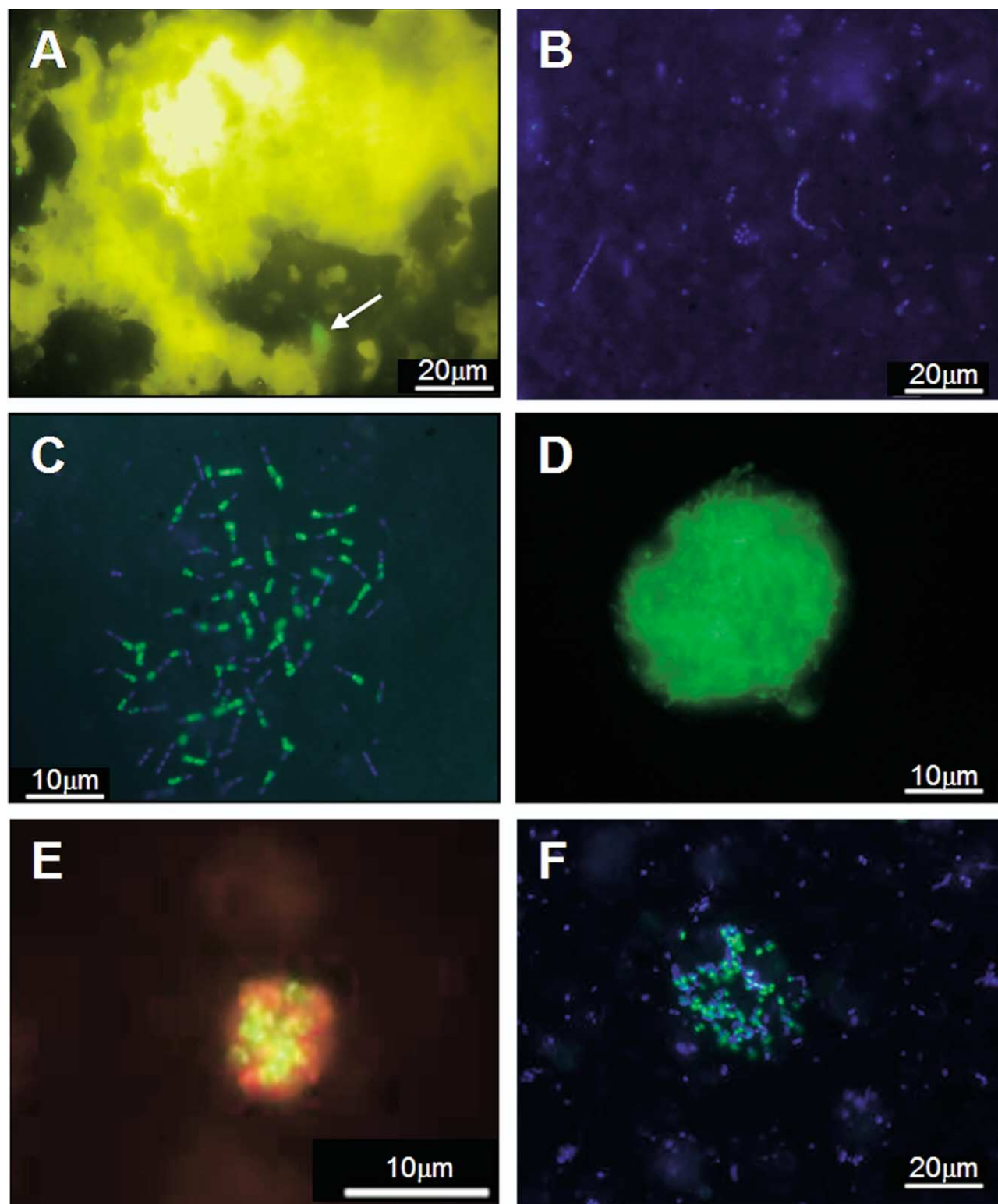


Fig. 3. Photomicrographs of microorganisms in Gulf of Mexico sediments identified using CARD-FISH. Scale bars represent various lengths. (A) Oil autofluorescence prevented robust usage of mono-labeled FISH probes. Arrow indicates a cell targeted by a general *Archaeal* rRNA FISH probe labeled with a green fluorescent dye to illustrate difficulty in separating signal from oil autofluorescence. (B) Representation of microbial morphologies present. Cells stained with DAPI (blue). (C) Loose cluster of rods targeted with green-fluorescent probe specific for the ANME-1 group of Archaea. Other rod-shaped cells in the image (stained with DAPI, blue) may be ANME with a low cellular rRNA content, making these cells fall below the threshold of detection for FISH. (D) Mono-specific cluster of microorganisms targeted with a green-fluorescent probe specific for the ANME-1 group of Archaea. No SRB of the *Desulfosarcina/Desulfococcus* group,

1B). Both acetate concentrations and rates of Ac-MOG were also low in these sediments (Fig. 1C). The SR rates, in contrast, were extremely high between 2 and 8 cm ( $>3.5 \mu\text{mol cm}^{-3} \text{d}^{-1}$ ; Fig. 1D). The sulfate concentration decreased from 26 to 15 mmol/L over 10 cm (Fig. 1D). Sulfide ( $\text{H}_2\text{S}$ ) gradually increased from 0.2 mmol/L at the surface to 7 mmol/L at 11 cm (Table 1). Although these sediments were collected from a brine seep, the pore water chlorinity ( $\text{Cl}^-$ ) did not increase markedly with depth (Table 1), showing that the core did not penetrate into brine. Averaged over the top 10 cm, AOM and SR rates were 0.1 and  $154 \text{ mmol m}^{-2} \text{d}^{-1}$ , respectively, and the Bi-MOG rate was  $4.8 \mu\text{mol m}^{-2} \text{d}^{-1}$ .

In contrast to the brine site, sediments collected from a gas hydrate site (GC232) contained significant concentrations of methane ( $<1.5 \text{ mmol/L}$ ; Fig. 2A), though still below in situ saturation values ( $\sim 80 \text{ mmol/L}$ ). The peak in methane concentration at 5 to 7 cm coincided with the peak in AOM ( $\sim 160 \text{ nmol cm}^{-3} \text{d}^{-1}$ ; Fig. 2A) and Bi-MOG ( $\sim 30 \text{ nmol cm}^{-3} \text{d}^{-1}$ ; Fig. 2B). The  $\text{HCO}_3^-$  concentration increased rapidly from the surface ( $<2 \text{ mmol/L}$ ) to 5 to 7 cm where concentrations were  $\sim 30 \text{ mmol/L}$  (Fig. 2B). Acetate concentration, in contrast, remained fairly constant ( $<12 \mu\text{mol/L}$ ) down to 5 to 7 cm, then increased dramatically to  $\sim 400 \mu\text{mol/L}$  at 15 cm (Fig. 2C). Similarly, Ac-MOG was negligible ( $<0.1 \text{ nmol cm}^{-3} \text{d}^{-1}$ ) above 5 to 7 cm, but increased gradually to  $>50 \text{ nmol cm}^{-3} \text{d}^{-1}$  by 15 cm (Fig. 2C). Sulfate was rapidly consumed within 0 to 4 cm from 28 to  $\sim 6 \text{ mmol/L}$  and then gradually decreased between 4 and 10 cm (Fig. 2D). Rates of SR ranged from 80 to  $640 \text{ nmol cm}^{-3} \text{d}^{-1}$  in the upper 10 cm, and were usually greater than AOM rates (Fig. 2D). The SR rates in deeper sediments were extremely high ( $>3.3 \mu\text{mol cm}^{-3} \text{d}^{-1}$ ; Fig. 2D). Overall concentrations of  $\text{H}_2\text{S}$  were high ( $>11 \text{ mmol/L}$ ) throughout the core, with a peak in concentration ( $\sim 20 \text{ mmol/L}$ ) at 5 cm (Table 1). A noticeable decrease in  $\text{Cl}^-$  from 557 mmol/L at the surface to 421 mmol/L at 7 cm (Table 1) in the core suggests freshening of the porewater, possibly via gas hydrate dissociation during core recovery. Aerial AOM and SR rates at GC232 in the upper 10 cm were 6.4 and  $\sim 30 \text{ mmol m}^{-2} \text{d}^{-1}$ , respectively; Bi-MOG and Ac-MOG rates were  $\sim 380$  and  $93.2 \mu\text{mol m}^{-2} \text{d}^{-1}$ , respectively.

### 3.2. Distribution and Diversity of Microorganisms

Using CARD-FISH, we evaluated the abundance patterns of five groups of prokaryotes. Total cell counts via AODC were higher in brine sediments ( $5.6 \pm 0.7 \times 10^9 \text{ cells ml}^{-1}$ ) than in gas hydrate sediments ( $2.7 \pm 0.7 \times 10^9 \text{ cells ml}^{-1}$ ; Table 1). In brine sediments, *Bacteria* dominated the surficial microbial community; however, below 5 cm, *Archaea* abundance increased significantly, accounting for nearly 50% of the total microbial population at 9 cm (Table 1). In contrast, *Bacteria*

were dominant over depth in hydrate sediments, although the proportion of *Archaea* increased with depth (Table 1).

CARD-FISH with group specific primers revealed high numbers of putative methanotrophic archaea (i.e., ANME-1 and ANME-2; Figs. 1E and 2E; Table 1), although the abundance patterns were noticeably different between sites. At the brine site, ANME-1 dominated the archaeal microbial population below 3 cm, increasing from 12% to 46% of the total microbial community (70%–95% of *Archaea*) within the zone where peak SR activity was observed (Fig. 1E). Typically, ANME-1 occurred as short rods (2–3  $\mu\text{m}$  in length) or as segmented rod chains consisting of two to eight cells up to 20  $\mu\text{m}$  in length (Fig. 3C); mono-specific clusters of ANME-1 up to 25  $\mu\text{m}$  in diameter were also observed (Fig. 3D). Although not present in high abundance, ANME-2 archaea were typically found in shell-type consortia with sulfate reducing bacteria (SRB) of the *Desulfosarcina/Desulfococcus* spp. (DSS) taxon (Figs. 1E and 3E). Clusters ranged from 5 to 25  $\mu\text{m}$  in diameter. ANME-1 occasionally formed loose clusters with other microorganisms, including DSS and other unidentified bacteria. DSS-type cells were most often found associated with ANME-2 cells in shell-type consortia.

In gas hydrate sediments, ANME-1 was also the dominant archaeal group (Fig. 2E, Table 1), accounting for up to 20% of the total microbial population and 78% of total *Archaea* at depth. Shell-type consortia of the ANME-2/DSS were more abundant and generally larger in size at the gas hydrate site. DSS-targeted cells were often found unassociated with either of the ANME groups; these microbes had a vibrio-like morphology in contrast to the more coccoid-like DSS-SRB that were observed in the ANME consortia. ANME-2 were not observed in shell-type consortia with non-DSS cells, although they were occasionally observed in loose arrangements without associated DSS (Fig. 3F). Both ANME populations increased around the depth where rates of AOM and Bi-MOG peaked; DSS increased in the same interval (Fig. 2E). At this depth, combined numbers of ANME-1 and ANME-2 comprised  $>96\%$  of the total *Archaea*.

### 3.3. Distribution and C Isotopic Signatures of Lipid Biomarkers

The abundance and C isotopic composition of signature lipid biomarkers were evaluated to infer carbon flow through the microbial population. Unraveling carbon flow in such complex systems requires knowledge of the isotopic values of various carbon pools (for example, methane, carbon dioxide, organic acids, organic matter, etc.; Table 2). The  $\delta^{13}\text{C}$ -methane at the brine site was  $\sim 14\%$  to 30% lighter than that observed at the hydrate site. Values of  $\delta^{13}\text{C}$  for acetate or other labile organic acids (common substrates for sulfate reducers) are, to our knowledge, unknown at either site.

---

which were targeted with a red-fluorescent probe, were visible in this cluster. (E) Organized consortia of ANME-2 (targeted with a group specific green-fluorescent probe) and *Desulfosarcina/Desulfococcus* spp. (targeted with a group-specific red-fluorescent probe). ANME-2 were typically found in organized consortia with these SRB. (F) Loose cluster of ANME-2 cells (green) surrounded by other microorganisms which were not related to the *Desulfosarcina/Desulfococcus* spp. (which would have been labeled red).

Table 2. Isotopic composition of various carbon compounds from gas hydrate and brine pool sites in the Gulf of Mexico.

Compound	Gas hydrate	Brine pool
Methane	$\delta^{13}\text{C}$ (‰) <sup>a</sup>	$\delta^{13}\text{C}$ (‰)
Vent gas	-48.5 <sup>b</sup>	-63.8 to -80 <sup>b</sup>
Hydrate-bound	-47.5 <sup>b</sup>	
Porewater	-49.3 <sup>b</sup>	
Particulate organic matter	-25 <sup>c</sup>	-25 <sup>i</sup>
Sedimentary carbonate	-15 to -26 <sup>d</sup>	-10 <sup>i</sup>
Dissolved inorganic carbon	-30 <sup>b</sup>	
C <sub>22</sub> -C <sub>30</sub> alkanes (average)	-30.1 <sup>e</sup>	
Photic zone organic matter	-20.6 <sup>f</sup>	
Crude oil	-27 <sup>g</sup>	

<sup>a</sup> Isotopic composition versus the Vienna Pee Dee belemnite standard.

<sup>b</sup> From site GC234, ~9.5 km from the site in this study (Sassen et al., 2004).

<sup>c</sup> From site GC185 (Joye et al., 2004).

<sup>d</sup> From site GC234 (Formolo et al., 2004; Joye et al., 2004).

<sup>e</sup> Jahnke et al. (1995).

<sup>f</sup> Claypool and Kaplan (1974).

<sup>g</sup> Kennicutt et al. (1988).

<sup>h</sup> Same brine pool as this study, GC233 (MacDonald, 2002; MacDonald et al., 1990b).

<sup>i</sup> Same brine pool as this study, GC233 (Joye et al., 2004).

Lipid biomarkers diagnostic for the putative methanotrophic archaea (i.e., archaeol and *sn*-2-hydroxyarchaeol; Elvert et al., 1999; Hinrichs et al., 1999; Orphan et al., 2002) were present at low concentration at both sites (Figs. 1F and 2F, Tables 3A and 3B). These biomarkers were very depleted in <sup>13</sup>C, with  $\delta^{13}\text{C}$  values of -90.7‰ to -114.5‰ at the brine site (Fig. 1G, Table 3A) and -83.9‰ to -104.6‰ at the gas hydrate site (Fig. 2G, Table 3B). Generally, stronger <sup>13</sup>C-depletions and higher concentrations were detected for *sn*-2-hydroxyarchaeol at both sites with the exception of two depths at the brine site, where archaeol was more <sup>13</sup>C-depleted. Other forms of hydroxyarchaeol were not detected at either site. Signature archaeal hydrocarbon lipids could not be analyzed due to weak signal-to-noise resolution of lipids against a strong background of an unresolved complex mixture (UCM; Zhang et al., 2002). Other important membrane lipids such as glycerol dialkyl glycerol diethers (GDGTs) and their biphytanic hydrocarbon degradation products (Hinrichs et al., 2000; Pancost et al., 2001; Blumenberg et al., 2004) were not targeted by the methods employed here.

In brine sediments, the most abundant bacterial fatty acid, *cis*-11 octadecanoate (18:1 $\omega$ 7c; Table 3A), had  $\delta^{13}\text{C}$  values

Table 3A. Abundance (expressed as  $\mu\text{g}$  lipid  $\text{g}^{-1}$  sediment) and isotopic composition ( $\delta^{13}\text{C}$  vs. PDB standard) of select lipid biomarkers extracted from sediments at a brine influence site in the Gulf of Mexico. See text for explanation of lipid nomenclature.

Location	Lipid	0-2 cm		2-4 cm		4-6 cm		6-8 cm		8-10 cm	
		$\mu\text{g}/\text{g}$	$\delta^{13}\text{C}$	$\mu\text{g}/\text{g}$	$\delta^{13}\text{C}$	$\mu\text{g}/\text{g}$	$\delta^{13}\text{C}$	$\mu\text{g}/\text{g}$	$\delta^{13}\text{C}$	$\mu\text{g}/\text{g}$	$\delta^{13}\text{C}$
GC233	14:0 <sup>a</sup>	10.5	—	5.7	58.5	2.5	—	1.2	—	0.9	—
	i15:0	5.3	—	2.3	—	1.2	—	0.9	—	0.5	—
Brine pool	a15:0	9.6	41.9	5.0	48.0	3.1	58.9	3.2	62.9	2.9	68.9
	15:0	2.1	—	1.3	—	0.6	—	0.7	—	0.4	—
	16:1 $\omega$ 7c	11.5	45.2	4.6	56.3	10.2	61.1	6.4	83.3	2.7	57.5
	16:1 $\omega$ 5c	20.7	43.4	11.0	47.4	3.3	55.6	2.7	66.4	1.1	71.9
	16:0	41.2	62.6	19.5	65.8	7.4	72.1	7.0	—	4.7	90.4
	10Me16:0	5.3	40.6	3.5	40.4	0.7	37.7	0.5	31.3	n.d.	35.9
	17:1 $\omega$ 6c	1.7	53.1	1.1	64.3	1.0	62.6	1.0	65.1	0.5	n.d.
	cy17:0 $\omega$ 5,6	0.7	54.4	1.1	69.0	0.5	79.6	0.5	76.1	n.d.	79.1
	17:0	1.2	—	0.7	—	0.3	—	0.3	—	0.2	n.d.
	18:1 $\omega$ 9c	6.1	36.2	2.9	39.1	1.2	32.4	2.0	32.9	1.1	—
	18:1 $\omega$ 7c	43.8	37.4	21.2	39.7	9.3	40.2	8.5	46.2	5.2	38.3
	18:0	9.2	39.8	6.7	48.3	3.9	68.6	4.5	71.8	3.1	79.2
	Archaeol <sup>b</sup>	0.5	25.4	0.3	23.6	0.3	20.7	n.d.	22.5	0.3	—
	<i>sn</i> -2-hydroxy	1.1	100.5	0.6	114.5	0.7	109.5	n.d.	n.d.	0.2	93.2
			113.3		109.2		114.5				-90.7

n.d. = not detected; n.m. = not measurable due to low signal to noise ratio.

<sup>a</sup> Bacterial fatty acids.

<sup>b</sup> Archaeal alcohol lipids.

Table 3B. Abundance (expressed as  $\mu\text{g lipid g}^{-1}$  sediment) and isotopic composition ( $\delta^{13}\text{C}$  vs. PDB standard) of select lipid biomarkers extracted from sediments at a gas hydrate site in the Gulf of Mexico. See text for explanation of lipid nomenclature.

Location	Lipid	0–2 cm		2–4 cm		4–6 cm		6–8 cm		8–10 cm		
		$\mu\text{g/g}$	$\delta^{13}\text{C}$	$\mu\text{g/g}$	$\delta^{13}\text{C}$	$\mu\text{g/g}$	$\mu\text{g/g}$	$\delta^{13}\text{C}$	$\mu\text{g/g}$	$\delta^{13}\text{C}$	$\mu\text{g/g}$	
GC232	14:0 <sup>a</sup>	18	—	13.2	—	14.1	—	14.6	—	2.2	—	
	i15:0	16.9	—	11.2	—	9.4	—	8.3	—	1.1	—	
Gas hydrate	a15:0	31.5	—	28.1	—	22.9	—	21.4	—	3.6	—	
	15:0	5.4	—	3.8	—	3.6	—	4.8	—	0.7	—	
	16:1 $\omega$ 7c	344	—	63.3	—	51.8	—	36.1	—	4.1	—	
	16:1 $\omega$ 5c	26.8	—	15.2	—	15.7	—	16.2	—	2.3	—	
	16:0	87	—33	40.4	—	29.9	—	26.5	—	8.6	—	
	10Me16:0	3.1	—	2.9	—	5.2	—	4.5	—	0.4	—	
	17:1 $\omega$ 6c	3.4	—	2.4	—	2.1	—	5.6	—	0.9	—	
	cy17:0 $\omega$ 5,6	0.8	—	1.5	—	2.9	—	5.4	—	1.2	—	
	17:0	3.4	—	1.9	—	1.5	—	1.5	n.m.	0.5	—	
	18:1 $\omega$ 9c	14.6	—	9.7	—	6.5	—	5.2	—	1.3	—	
	18:1 $\omega$ 7c	124.2	—30.2	31.6	—43.8	27.1	—46.8	32.0	—63.6	6.2	—70.1	
	18:0	17.1	—	13.7	—	9.1	—	8.1	—	11	—	
	Archaeol <sup>b</sup>	n.d.	n.d.	1.2	—	1.9	—	3.2	—	1.9	—	
	sn-2-hydroxy	n.d.	n.d.	1.7	—	1.3	—97	9.3	—	2.9	—104.6	
					102.6				101.5			

n.d. = not detected; n.m. = not measurable due to low signal to noise ratio.

<sup>a</sup> Bacterial fatty acids.

<sup>b</sup> Archaeal alcohol lipids.

ranging from  $-39.8\text{‰}$  at the surface to  $-79.2\text{‰}$  at 10 cm. After the generic bacterial biomarker hexadecanoate (16:0), the unsaturated lipids cis-11 hexadecanoate (16:1 $\omega$ 5c) and cis-9 hexadecanoate (16:1 $\omega$ 7c) were most abundant (Table 3A). 16:1 $\omega$ 5c, a biomarker diagnostic for DSS in the AOM consortia (Elvert et al., 2003), had  $\delta^{13}\text{C}$  values ranging from  $-62.6\text{‰}$  at the surface to  $-90.4\text{‰}$  at depth (Figs. 1H and II, Table 3A). The branched chain 13-methyltetradecanoate (ai-15:0) and 12-methyltetradecanoate (i-15:0) fatty acids (Figs. 1H and II, Table 3A), both considered generally diagnostic for sulfate reducing bacteria (Taylor and Parkes, 1985), also exhibited  $^{13}\text{C}$  depletion with increasing depth (down to  $-83.7\text{‰}$  for ai-15:0 and  $-68.9\text{‰}$  for i-15:0). Although in low abundance, two additional fatty acids showed significant depletion in  $^{13}\text{C}$  with depth: the cyclopropane fatty acid 11,12-methylene-hexadecanoic acid (cy17:0 $\omega$ 5,6) exhibited  $\delta^{13}\text{C}$  values from  $-73.8$  to  $-112.4\text{‰}$  and cis-11 heptadecanoate (17:1 $\omega$ 6c) exhibited a  $\delta^{13}\text{C}$  range of  $-54.4\text{‰}$  to  $-79.6\text{‰}$  (Table 3A). Both of these lipids are suggested to be indicative of the DSS involved in AOM (Elvert et al., 2003). Recent evidence suggests that the occurrence of 16:1 $\omega$ 7c, 16:1 $\omega$ 5c, and cy17:0 $\omega$ 5,6 fatty acids may also be indicative of DSS associated with ANME-2 ('ANME-2-type DSS'), while isotopically  $^{13}\text{C}$ -depleted ai15:0 and i15:0 lipids derive from DSS associated with ANME-1

('ANME-1-type DSS'; Blumenberg et al., 2004). The branched chain 15-methylhexadecanoate (ai-17:0) and 14-methylhexadecanoate (i-17:0) fatty acids were in very low abundance, and their values are not reported here.

Overall patterns of lipid abundance were similar in gas hydrate sediments, with a few notable exceptions. 16:1 $\omega$ 7c was the most abundant biomarker, followed by 18:1 $\omega$ 7c; both showed depletion in  $^{13}\text{C}$  with depth (Table 3B). Of the biomarkers supposedly diagnostic for SRB, ai-15:0, 16:1 $\omega$ 5c, and i-15:0 were the most abundant (Fig. 2H, Table 3B). As at the brine site, these fatty acids generally exhibited lighter  $\delta^{13}\text{C}$  values with depth, with 16:1 $\omega$ 5c having the strongest depletion ( $-67.6\text{‰}$ ; Fig. 2I, Table 3B). Cy17:0 $\omega$ 5,6 was more abundant at the gas hydrate site and was the most  $^{13}\text{C}$  depleted (down to  $-79.6\text{‰}$  at 4–6 cm depth; Figs. 2H and 2I, Table 3B). In general, both the bacterial fatty acids and the archaeal alcohol biomarkers were heavier at the hydrate-site than at the brine site (Tables 3A and 3B).

#### 4. DISCUSSION

This study presents the first data set from two distinct cold seeps comparing results from radiotracer-based measurements of AOM, MOG, and SR with geochemical, microbial diversity,

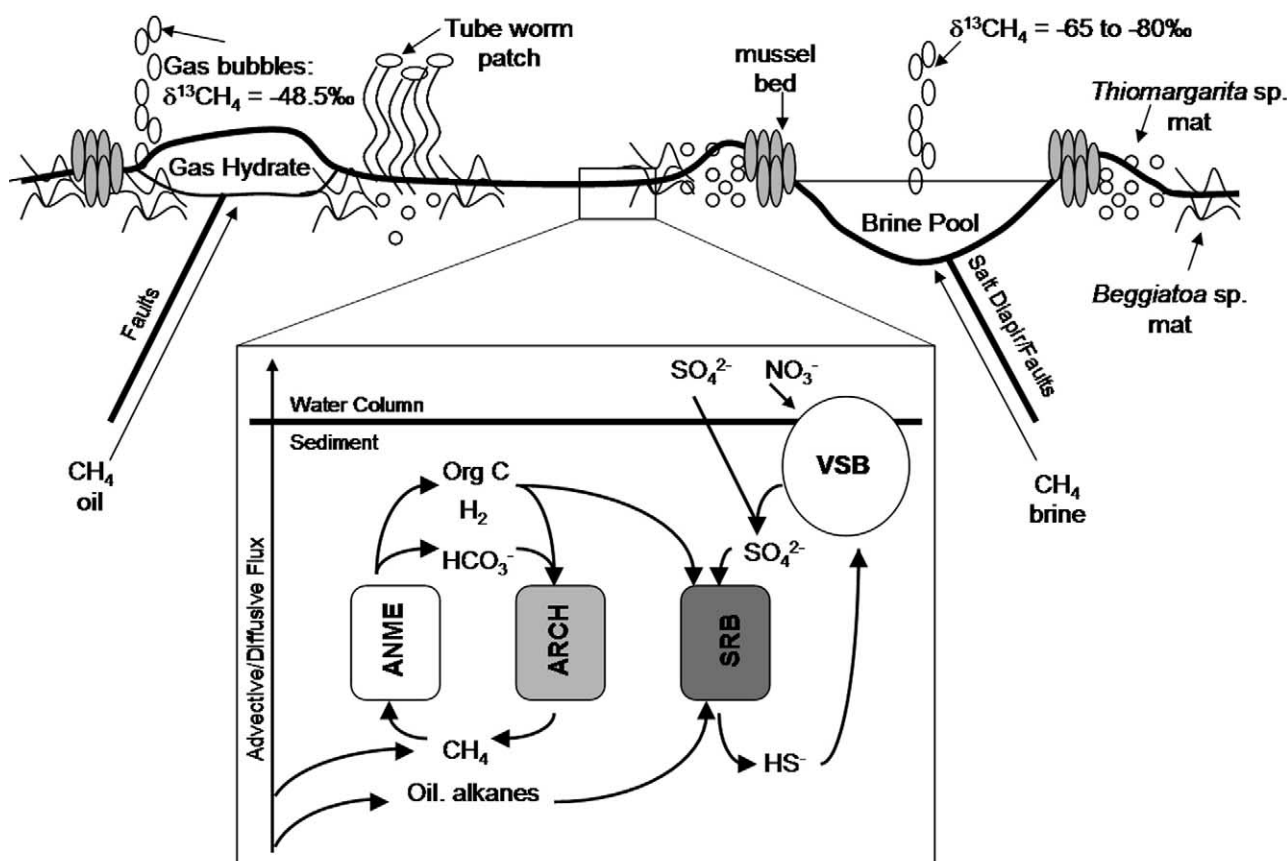


Fig. 4. Schematic illustrating the interactions between AOM, SR and MOG, the geochemical, and the geological environment at the two cold seep environments. Not drawn to scale. Macrofaunal and microbial mat communities are indicated by specific symbols labeled in the figure. The left-hand side of the diagram depicts a gas hydrate site (GC232) fed by methane and oil migrating through faults and fractures. The carbon isotopic composition of the mostly thermogenic source methane at this site is taken from Sassen et al. (2004). Surficial chemosynthetic communities at this site include *Beggiatoa* spp. and other sulfide oxidizing bacterial mats, tube worms and mussels. The right-hand side of the diagram illustrates a brine pool site (GC233), characterized by the migration of biogenic methane (MacDonald, 2002) and brines, with a surface chemosynthetic community composed of mussels and *Thiomargarita*-type sulfide oxidizing bacterial mats. The inset shows a magnified view of hypothesized cycling of methane and sulfur occurring in subsurface sediments mediated by ANME-type microorganisms (ANME), methanogenic archaea (ARCH; which could also be ANME, see text for explanation), sulfate reducing bacteria (SRB), and giant vacuolated sulfide oxidizing bacteria (VSB); arrows indicate the flow of various compounds between microorganisms and the environment.

and lipid biomarker data. We observed decoupling of SR from AOM as well as the contemporaneous production of methane from bicarbonate and the oxidation of methane to bicarbonate in sediments from gas hydrate and brine sites. Phylogenetic and organic geochemical evidence indicate that microbial groups associated with AOM coupled to SR (i.e., ANME-1, ANME-2, and DSS; Boetius et al., 2000; Hinrichs et al., 2000; Orphan et al., 2001b; Michaelis et al., 2002) were present in these sediments and ANMEs dominated the archaeal community. We suggest that both types of ANMEs were responsible for the observed <sup>14</sup>C-methane consumption and that one or both of the ANMEs were responsible for the observed methane production.

A schematic of physical and geochemical characteristics of the sites, highlighting the differences between the two cold seep environments, is presented in Figure 4. Interactions between AOM, SR and MOG occurring in sediments underlying microbial mats are also illustrated. The oxidation of methane by

ANME microorganisms is linked to sulfate reduction activity, although the specific intermediate coupling these processes is unknown. Other *Archaea*, perhaps ANME microorganisms, produce methane within the same environment, though the mechanism of potential coupling between MOG and AOM is unclear. Oxidation of oil and other alkanes may also fuel sulfate reduction activity, particularly at the gas hydrate site.

#### 4.1. Brine-Dominated Cold Seeps

The geochemical profiles in brine sediments (e.g., low methane and high sulfate concentrations at depth) showed that the "traditional" sulfate-methane interface, which demarcates the AOM zone, was not penetrated in this core. However, SR rates were extremely high (>3.5 μmol cm<sup>-3</sup> d<sup>-1</sup>, 154 mmol m<sup>-2</sup> d<sup>-1</sup> for the upper 10 cm), similar to previous SR rates documented in the Gulf of Mexico (Arvidson et al., 2004; Joye et

al., 2004) and higher than rates observed at other methane seeps (Hansen et al., 1998; Pimenov et al., 1999; Boetius et al., 2000; Weber and Jørgensen, 2002; Aharon and Fu, 2003; Treude, 2003; Treude et al., 2003). High SR and low AOM suggests that the majority of SR activity was fueled by organic carbon sources other than methane (Joye et al., 2004).

Despite the observed low rates of AOM in brine sediments, turnover of the methane pool was rapid ( $\sim 10\% \text{ d}^{-1}$ ; Fig. 1A), suggesting a considerable potential for AOM during periods of increased methane fluxes/concentrations. The conspicuously dominant ANME-1 population increased rapidly within and below the depth of maximal AOM and Bi-MOG rates. Given the observed low rate of AOM, the large size of the ANME population is surprising, suggesting that this population either used another metabolic strategy (see inset of Fig. 4), was supported by the measured (low) AOM rates, or reflected a previous high methane flux/methane oxidation activity period. The presence and  $^{13}\text{C}$  depletion of archaeal lipids indicated an active, or recently active, AOM-mediating population. Fluid flow through cold seep sediments is transient in both space and time (Linke et al., 1994; Brown et al., 1996; Tyron et al., 1999; Torres et al., 2002a). Currently, it is unclear how long populations of AOM-associated microbes can survive during periods of low methane flux. Available data indicate that anaerobic methanotrophs grow slowly (doubling time of several months; Nauhaus et al., 2002), even under relatively high methane concentrations, inferring that the modest energy yield of AOM results in low anabolic rates.

Though AOM rates were low, SR rates were extremely high. To reconcile the observed sulfate profile with the high SR rates (Fig. 1D) requires a sulfate source in addition to diffusion (Arvidson et al., 2004). Brine advection through the sediments would reduce the sulfate penetration depth since the brine contains no sulfate (Joye et al., 2005) and, at present, no fluid flux rates are available for this site. However, it is possible that brine advection generates convection cells that drive seawater percolation through sediments at the edge of the brine pool, increasing sulfate availability at least in some areas. Modeling of geochemical profiles at gas hydrate sites indicated that organism-sediment interactions replenish subsurface sulfate via bioirrigation and/or in situ recycling via anaerobic sulfide oxidation (Arvidson et al., 2004; Cordes et al., 2005) but tube-worms are not abundant at this brine pool. Some sulfide oxidizing microbes (e.g., *Thiovolulum*) common to sulfide-rich sediments generate structures (e.g., veils) that influence flow through the sediments to optimize geochemical conditions for their activity (Fenchel and Glud, 1998). *Beggiatoa* at Gulf of Mexico cold seeps also form complex surface veils that may influence fluid flow through sediments. The surface sediments at the brine site were covered by a dense mat of a giant sulfide oxidizing bacteria closely related to *Thiomargarita namibiensis* ( $0.51 \text{ mm}^3 \text{ cm}^{-3}$  biovolume; Kalenetra et al., 2005). However, because 99% of the sulfide oxidizing bacterial biomass was found in the upper 2 cm of sediment (Kalenetra et al., unpublished data) and because *Thiomargarita*-like microbes are not motile, it is unlikely that they supplied sulfate to depths  $> 5$  cm. One possible explanation for the increased sulfate concentration at depth is barite dissolution. Authigenic barite is abundant at cold seeps in the Gulf of Mexico (Fu et al., 1994) and elsewhere (Paytan et al., 2002; Torres et al., 2002b, 2003).

Similar increases in sulfate concentration at depth in cold seep sediments in the Sea of Okhotsk were linked to barite dissolution (Greinert et al., 2002). We hypothesize that barite dissolution is responsible for generating the increased sulfate concentration observed at depth and plan to address this possibility in future studies.

The abundance of *Thiomargarita*-related bacteria correlated with the lipid biomarker profiles of the sediments. The 18:1 $\omega$ 7c and 16:1 $\omega$ 7c fatty acids likely derive from *Beggiatoa* spp. (Cantu et al., 2003; Elvert et al., 2003). In the brine sediments, 18:1 $\omega$ 7c and 16:0, both having similar  $\delta^{13}\text{C}$ -values of  $\sim -40\text{‰}$ , were the dominant fatty acids; 16:1 $\omega$ 7c ( $-43\text{‰}$ ) was less common. Since *Beggiatoa* spp. were almost two orders of magnitude less abundant than the dominant *Thiomargarita namibiensis*-relative (Kalenetra et al., 2005), the 18:1 $\omega$ 7c  $> 16:1\omega 7c$  trend may reflect a biosignature of this abundant microbe.

Although the SR rate was high in brine sediments, the total number of SRB detected with CARD-FISH was low:  $< 7\%$  of cells were DSS (compared with 40%–50% ANME-1; Fig. 1E). The DSS 658 probe may not have targeted the dominant SRB in these sediments; however, hybridization with other FISH probes specific for putative seep-endemic SRB (probe DSR 651, *Desulforhopalus* spp.; probe 660, *Desulfobulbus* spp.; Knittel et al., 2003) revealed that these microorganisms were rare ( $< 5\%$  and 1%, respectively, of the total population; data not shown). Previous work at Gulf of Mexico gas hydrate sites (Lanoil et al., 2001; Mills et al., 2003, 2004) indicated that a significant fraction (32.4%) of  $\delta$ -*Proteobacteria* sequences in sediments (based on 16S complementary rDNA clone libraries; Mills et al., 2004) fall within the coverage of the DSS 658 probe, although  $\sim 49\%$  of  $\delta$ -*Proteobacteria* sequences (Mills et al., 2004) group with the “SEEP-SRB2/Eel-2 group” of SRB (Orphan et al., 2001a; Knittel et al., 2003), which is not targeted by the DSS 658 probe (Knittel et al., 2003) or any other published probe. To our knowledge, no  $\delta$ -*Proteobacteria* sequences have been published for Gulf of Mexico brine sediments; therefore, the SRB at these sites could be divergent from known groups and thus were not targeted by the FISH probes we used.

The DSS-cells observed in the brine sediments occurred almost exclusively in consortia arrangements with ANME-2 microorganisms. This association was also evident in the lipid biomarker profiles: in the upper depths of the sediment, the ANME-2-type DSS signature lipids (Blumenberg et al., 2004; Elvert et al., 2003) were abundant and significantly depleted in  $^{13}\text{C}$ . However, ANME-1-type DSS appeared to become more prevalent with depth (based on decreasing abundance of ANME-2-type DSS signature lipids and depletion of  $^{13}\text{C}$  of ANME-1-type DSS signature lipids; Figs. 1H and 1I, Table 3A). The concentration ratio of *sn*-2-hydroxyarchaeol to archaeol in the upper sediments indicates that the ANME-2 may be the dominant producer of these lipids (Blumenberg et al., 2004). In the upper sediment layers, ANME-2-type consortia carry the strongest AOM-derived signal, followed by ANME-1 with depth, a pattern consistent with other observations (Orphan et al., 2004).

#### 4.2. Gas Hydrate-Dominated Cold Seeps

In gas hydrate site sediments, the coincident occurrence of AOM and Bi-MOG was observed between 5 and 9 cm (Figs. 2A

and 2B). As observed at the brine site, total Bi-MOG rates were ~10% of AOM rates, although rates of both processes were 2 orders of magnitude higher at the hydrate site, where methane concentrations were also higher. Within the zone of elevated AOM and MOG, the populations of ANME-1, and to a lesser degree ANME-2, increased as based on CARD-FISH observations; together they comprised nearly 92% of the identified *Archaea* (Fig. 2E, Table 2). A study of sediments collected at a nearby gas hydrate site (GC234, 9.5 km from GC232) indicated that only the ANME-2 group was metabolically active (based on complementary rDNA clone libraries; Mills et al., 2004), even though ANME-1 comprised a significant portion of archaeal 16S rRNA clone libraries (17.2%, Lanoil et al., 2001; 19.8%, Mills et al., 2003). Since FISH methods are based on the presence of rRNA, a molecule that degrades rapidly in dead or dying microbial cells, our data suggest that both groups are metabolically active at these sites.

The higher abundance of ai15:0 and i15:0 in the hydrate site sediments suggest the association of DSS with ANME-1 (Blumenberg et al., 2004). Similarly, the abundance and <sup>13</sup>C-depletion of 16:1ω5c and cy17:0ω5,6 lipids may imply associations of DSS with ANME-2. Although the branched chain fatty acids were present in high concentration in the gas hydrate site sediments (specifically ai15:0 and i15:0), they were not the most <sup>13</sup>C depleted fatty acids observed (Fig. 2H, Table 3B), contrary to previous reports for Gulf of Mexico cold seep sediments (Zhang et al., 2002). The differences in lipid distributions and isotopic composition of bacterial biomarkers between brine and hydrate sediments most likely reflects the variability between the SRB populations (e.g., ANME-1-type or ANME-2-type DSS or other sulfate reducers), metabolism (e.g., involvement in AOM vs. oil, hydrocarbon or other DOM oxidation), and/or differences in available organic carbon substrates (e.g., absence of oil and higher alkanes at the brine site). Overall, the isotopic composition of DSS lipids are relatively heavy at the hydrate site, which is consistent with the incorporation of carbon derived from heavier thermogenic methane or fractionation during lipid biosynthesis.

In contrast to the brine sediments, in gas hydrate site sediment, DSS-type SRB were abundant (≤20% with depth, Fig. 2E). Many of the observed DSS were attached to ANME-2 archaea in consortia of various sizes (Fig. 3E); however, the majority occurred alone or in loose association with ANME-1 or other unidentified bacteria. The unattached DSS-SRB typically had a vibrio-like morphology when compared to the coccoid DSS-SRB noted in consortia with ANME-2, suggesting that distinct subpopulations of DSS-type SRB inhabited the gas hydrate site sediment. As observed in brine sediments, only a few cells could be visualized with FISH probes for other non-DSS SRB (i.e., *Desulforhopalus*, *Desulfobulbus* spp.; data not shown). The unattached DSS-SRB and possibly other SRBs likely contributed to the high SR observed; the excess SR activity (relative to AOM) was probably coupled to oxidation of higher hydrocarbons or oil (Joye et al., 2004).

In the surficial sediments from the hydrate site, which were covered by a mat containing white *Beggiatoa* and other sulfide oxidizing bacteria (Fig. 4), 16:1ω7c and 18:1ω7c were by far the most abundant fatty acids, with 16:1ω7c almost three times as abundant as 18:1ω7c (Table 3B). These lipids are suggested to be derived from sulfide oxidizing bacteria (Cantu et al.,

2003; Elvert et al., 2003). However, the lighter isotopic composition of 16:1ω7c (−63‰) compared to 18:1ω7c (−30‰) suggest that these fatty acids are derived from at least two different bacterial sources.

### 4.3. Are Methane Production and Oxidation Linked in AOM Zones?

Although there are substantial geochemical and geological differences between the two sites investigated in this study (highlighted in Fig. 4), similar trends of AOM and MOG activity were observed. In sediments from both sites, rates of Bi-MOG were ~10% of measured AOM rates within the zones of maximal activity. This contemporaneous occurrence of AOM and MOG, coupled with the observation that ANME-1, and to a lesser degree ANME-2, microorganisms dominated the archaeal community, suggests that one or both of the ANME groups catalyzes both processes (inset of Fig. 4). Previous studies with methanogenic cultures and methanogenic coastal sediments showed low rates of AOM relative to Bi-MOG (~1%–10% respectively; Hoehler et al., 1994; Zehnder and Brock, 1980). The coincident occurrence of AOM and Bi-MOG in sediments dominated by ANME's has been observed elsewhere (e.g., ANME-1 dominated Black Sea mats and ANME-2 dominated estuarine sediments; Treude, 2003), suggesting that the involvement of ANME's in AOM and MOG is widespread. Previous evidence suggests that ANME-1 may occur without associated sulfate reducing bacterial partners (Orphan et al., 2002) and the results presented here suggests that ANMEs may mediate MOG.

Recent evidence suggests that the ANME archaea contain genes involved in the methanogenic pathway and that expression of these genes generates catalytically active enzymes (Hallam et al., 2003, 2004; Krüger et al., 2003). These data help explain the biochemical machinery necessary to allow ANME's to oxidize methane (i.e., by reversing the methanogenic enzymatic machinery). However, if the enzymatic machinery is reversible, it is possible that the observed rates of MOG occur via enzymatic back-reaction (e.g., equilibrium enzyme effects). While it is highly unlikely that a single microorganism would both oxidize and produce methane for energy generation, it is possible that separate but similar microbes exploit opposing methanogenic/methanotrophic machinery depending on environmental geochemical cues and/or the association of syntrophic partners. An enzymatic back reaction with one pathway being dominant and the other representing a small fraction of the other could occur, as has been demonstrated in methanogens that oxidize methane slowly (~1%) relative to the rate of MOG (Zehnder and Brock, 1980; Hoehler et al., 1994). Availability of labile organic carbon, hydrogen, and other possible intermediates represent chemical cues that could influence the patterns of AOM coupled to MOG and SR. Determining which cues drive AOM-associated microbes to be net methanogenic vs. net methanotrophic is imperative to understand interactions between the microbes involved in AOM.

The observation that ANME-type microorganisms dominate the archaeal community in areas with coincident AOM and Bi-MOG raises questions about the function(s) of these microorganisms in the environment. Previous work (Pancost et al.,

2000; Orphan et al., 2001a, 2002, 2004; Teske et al., 2002) suggests that multiple and diverse groups of microorganisms are involved in AOM; the data presented here suggests that these microorganisms utilize multiple and diverse metabolic strategies (i.e., ANME-1 may be involved in MOG; Fig. 4). Presumably, microorganisms involved in AOM survive on the edge of thermodynamic limits since the energy yield of the net process is small (Hoehler et al., 1994; Sørensen et al., 2001), thus, it would be advantageous if they were able to utilize multiple metabolic strategies as a function of local environmental conditions. If ANME microorganisms mediate AOM by a reversal of the methanogenic pathway (Fig. 4; Zehnder and Brock, 1980; Hoehler et al., 1994; Hallam et al., 2003, 2004), the key, then, is to determine the factors that trigger the enzymatic processes to result in net methanotrophy vs. net methanogenesis. Achieving this goal requires additional research in a variety of environments where AOM occurs.

**Acknowledgments**—The authors thank the crew of the *R/V Seward Johnson II* and the *Johnson Sea Link II* submersible and the science party of the LExEn 2002 research cruise for their help in collecting and processing samples. We thank M. Erickson, K. Kalenetra, T. Lösekann, N. Finke, A. Perenthaler, and R. Amann for providing analytical assistance and expertise, J. Montoya for assistance with the conceptual development of Figure 4, and J. Harmmeijer and two anonymous reviewers for providing useful comments on this manuscript. This research was supported by the National Science Foundation Life in Extreme Environments Program (OCE-0085549) and by the American Chemical Society (PRF-36834-AC2). The U.S. Department of Energy and the NOAA-National Undersea Research Program provided funding for submersible operations. Financial support for B. Orcutt was provided by a University of Georgia graduate recruiting fellowship and by a National Science Foundation graduate fellowship.

*Associate editor:* J. P. Amend

## REFERENCES

- Aharon P. (1994) Geology and biology of modern and ancient submarine hydrocarbon seeps and vents: An introduction. *Geo-Mar. Lett.* **14**, 69–73.
- Aharon P. and Fu B. (2003) Sulfur and oxygen isotopes of coeval sulfate-sulfide in pore fluids of cold seep sediments with sharp redox gradients. *Chem. Geol.* **195**, 201–218.
- Albert D. B. and Martens C. S. (1997) Determination of low-molecular-weight organic acid concentrations in seawater and porewater samples via HPLC. *Mar. Chem.* **56**, 27–37.
- Alperin M. J. and Reeburgh W. S. (1988) Carbon and hydrogen isotope fractionation resulting from anaerobic methane oxidation. *Global Biogeochem. Cycles* **2**, 3, 279–288.
- Amann R., Krumholz L., and Stahl D. A. (1990) Fluorescent-oligonucleotide probing of whole cells for determinative, phylogenetic and environmental studies in microbiology. *J. Bacteriol.* **172**, 762–770.
- Arvidson R. S., Morse J. W., and Joye S. B. (2004) The sulfur biogeochemistry of chemosynthetic cold seep communities, Gulf of Mexico, USA. *Mar. Chem.* **87**, 97–119.
- Barnes R. O. and Goldberg E. D. (1976) Methane production and consumption in anaerobic marine sediments. *Geology* **4**, 297–300.
- Behrens E. Q. (1988) Geology of a continental slope oil seep, northern Gulf of Mexico. *Bull. Am. Assoc. Petrol. Geol.* **72**, 105–114.
- Blumenberg M., Seifert R., Reitner J., Pape T., and Michaelis W. (2004) Membrane lipid patterns typify distinct anaerobic methanotrophic consortia. *Proc. Natl. Acad. Sci. U.S.A.* **101**, 30, 11111–11116.
- Boetius A., Ravensschlag K., Schubert C. J., Rickert D., Widdel F., Gieseke A., Amann R., Jørgensen B. B., Witte U., and Pfannkuche O. (2000) A marine microbial consortium apparently mediating anaerobic oxidation of methane. *Nature* **407**, 623–626.
- Brown K. M., Bangs N. L., Froelich P. N., and Kvenvolden K. A. (1996) The nature, distribution and origin of gas hydrate in the Chile Triple Junction region. *Earth Planet. Sci. Lett.* **19**, 471–483.
- Canfield D. E., Raiswell R., Westrich J. T., Reaves C. M., and Berner R. A. (1986) The use of chromium reduction in the analysis of reduced inorganic sulfur in sediments and shale. *Chem. Geol.* **54**, 149–155.
- Cantu J., Zhang C. L., Huang Z., Pancost R. D., Lyons T. W., Formolo M. J., and Sassen R. (2003) Biogeochemical signatures and community structure of a microbial (*Beggiatoa*) mat in the gas hydrate system of Gulf of Mexico. *Geological Society of America Annual Meeting 2003, Abstract with Programs*, 619.
- Claypool G. E. and Kaplan I. R. (1974) The origin and distribution of methane in marine sediments. In *Natural Gases in Marine Sediments* (ed. I. R. Kaplan), pp. 99–139. Plenum, New York.
- Cordes E. E., Authur M. A., Shea K., Arvidson R. S., and Fisher C. R. (2005) Modeling the mutualistic interactions between tubeworms and microbial consortia. *PLoS Biol.* **3**, 3, e77, doi:10.1371/journal.pbio.0030077.
- Cragg B. A., Parkes R. J., Fry J. C., Herbert R. A., Wimpenny J. W. T., and Getliff J. M. (1990) Bacterial biomass and activity profiles within deep sediment layers. In *Proceedings of the Ocean Drilling Program, Scientific Results, Leg 112, Vol. 112* (eds. E. Suess and R. von Huene), pp. 607–619. Ocean Drilling Program.
- Crill P. M. and Martens C. S. (1986) Methane production from bicarbonate and acetate in an anoxic marine sediment. *Geochim. Cosmochim. Acta* **50**, 9, 2089–2097.
- Daims H., Bruhl A., Amann R., Schleifer K.-H., and Wagner M. (1999) The domain-specific probe EUB338 is insufficient for the detection of all Bacteria: Development and evaluation of a more comprehensive probe set. *Syst. Appl. Microbiol.* **22**, 434–444.
- De Beukelaer S. M., MacDonald I. R., Guinasso N. L., and Murrery J. A. (2003) Distinct side-scan sonar, RADARSAT SAR and acoustic profiler signatures of gas and oil seeps on the Gulf of Mexico slope. *Geo-Mar. Lett.* **23**, 3–4, 177–186.
- Devol A. H., Anderson J. J., Kuivila K., and Murrery J. W. (1984) A model for coupled sulfate reduction and methane oxidation in the sediments of Saanich Inlet. *Geochim. Cosmochim. Acta* **48**, 993–1004.
- Dickens G. R. (2001) The potential volume of oceanic methane hydrates with variable external conditions. *Org. Geochem.* **32**, 10, 1179–1193.
- Elvert M., Suess E., and Whiticar M. J. (1999) Anaerobic methane oxidation associated with marine gas hydrates: Super-light C-isotopes from saturated and unsaturated c-20 and c-25 irregular isoprenoids. *Naturwissenschaften* **86**, 295–300.
- Elvert M., Boetius A., Knittel K., and Jørgensen B. B. (2003) Characterization of specific membrane fatty acids as chemotaxonomic markers for sulfate-reducing bacteria involved in anaerobic oxidation of methane. *Geomicrobiol. J.* **20**, 403–419.
- Elvert M., Greinert J., Suess E. and Whiticar M. J. (2001) Carbon isotopes of biomarkers derives from methane-oxidizing microbes at Hydrate Ridge, Cascadia convergent margin. In *Natural Gas Hydrates: Occurrence, Distribution and Dynamics, Vol. 124* (eds. C. K. Paull and W. P. Dillon), pp. 115–129. American Geophysical Union.
- Fenchel T. and Glud R. N. (1998) Veil architecture in a sulphide-oxidizing bacterium enhances countercurrent flux. *Nature* **394**, 367–369.
- Formolo M. J., Lyons T. W., Zhang C. L., Kelley C., Sassen R., Horita J., and Cole D. R. (2004) Quantifying carbon sources in the formation of authigenic carbonates at gas hydrate sites in the Gulf of Mexico. *Chem. Geol.* **205**, 253–264.
- Fossing H. and Jørgensen B. B. (1989) Measurement of bacterial sulfate reduction in sediments—Evaluation of a single-step chromium reduction method. *Biogeochemistry* **8**, 205–222.
- Fu B., Aharon P., Byerly G. R., and Roberts H. H. (1994) Barite chimneys on the Gulf of Mexico continental slope: Initial report on their petrography and geochemistry. *Geo-Mar. Lett.* **14**, 2–3, 81–87.
- Gelwicks J. T., Risatti J. B., and Hayes J. M. (1994) Carbon-isotope effects associated with aceticlastic methanogenesis. *Appl. Environ. Microbiol.* **60**, 2, 467–472.
- Greinert J., Bollwerk S. M., Derkachev A., Bohrmann G., and Suess E. (2002) Massive barite deposits and carbonate mineralization in the

- Derugin Basin, Sea of Okhotsk: Precipitation processes at cold seep sites. *Earth Planet. Sci. Lett.* **203**, 165–180.
- Hallam S. J., Girguis P. R., Preston C. M., Richardson P. M., and Delong E. F. (2003) Identification of methyl coenzyme M reductase A (*mcrA*) genes associated with methane-oxidizing archaea. *Appl. Environ. Microbiol.* **69**, 9, 5483–5491.
- Hallam S. J., Putnam N., Preston C. M., Detter J. C., Rokhsar D., Richardson P. M., and Delong E. F. (2004) Reverse methanogenesis: Testing the hypothesis with environmental genomics. *Science* **305**, 1457–1462.
- Hansen L. B., Finster K., Fossing H., and Iversen N. (1998) Anaerobic methane oxidation in sulfate depleted sediments: Effects of sulfate and molybdate additions. *Aquat. Microb. Ecol.* **14**, 195–204.
- Hesselbo S. P., Groecke D. R., Jenkyns H. C., Bjerrum C. J., Farrimond P., Morgans Bell H. S., and Green O. R. (2000) Massive dissociation of gas hydrate during a Jurassic oceanic anoxic event. *Nature* **406**, 392–395.
- Hinrichs K.-U. and Boetius A. (2002) The anaerobic oxidation of methane: New insights in microbial ecology and biogeochemistry. In *Ocean Margin Systems* (eds. G. Wefer, D. Billett, D. Hebbeln, B. B. Jørgensen, M. Schlüter, and T. C. E. van Weering), pp. 457–477. Springer-Verlag, Berlin, Germany.
- Hinrichs K.-U., Hayes J. S., Sylva S. P., Brewer P. G., and Delong E. F. (1999) Methane-consuming archaeobacteria in marine sediments. *Nature* **398**, 802–805.
- Hinrichs K.-U., Summons R. E., Orphan V. J., Sylva S. P., and Hayes J. M. (2000) Molecular and isotopic analysis of anaerobic methane-oxidizing communities in marine sediments. *Org. Geochem.* **31**, 1651–1701.
- Hoehler T. M., Alperin M. J., Albert D. B., and Martens C. S. (1994) Field and laboratory studies of methane oxidation in an anoxic marine sediment—Evidence for a methanogen-sulfate reducer consortium. *Global Biogeochem. Cycles* **8**, 451–463.
- Hopman A. H., Ramaekers F. C., and Speel E. J. (1998) Rapid synthesis of biotin-, digoxigenin-, trinitrophenyl- and fluorochrome-labeled tyramides and their application for in situ hybridization using CARD amplification. *J. Histochem. Cytochem.* **46**, 6, 771–777.
- Intergovernmental Panel on Climate Change (2000) *Land Use, Land-Use Change, and Forestry. A Special Report of the Intergovernmental Panel on Climate Change (IPCC)* (eds. R. T. Watson, I. R. Noble, B. Bolin, N. H. Ravindranath, D. J. Verardo, and D. J. Dokken). Cambridge University Press, Cambridge, UK.
- Iversen N. and Jørgensen B. B. (1985) Anaerobic methane oxidation rates at the sulfate-methane transition in marine sediments from Kattekat and Skagerrak (Denmark). *Limnol. Oceanogr.* **30**, 944–955.
- Jahnke L. L., Summons R. E., Dowling L. M., and Zahirais K. D. (1995) Identification of methanotrophic lipid biomarkers in cold-seep mussel gills: Chemical and isotopic analysis. *Appl. Environ. Microbiol.* **61**, 2, 576–582.
- Jørgensen B. B. (1978) A comparison of methods for quantification of bacterial sulfate reduction in coastal marine sediments. I. Measurements with radiotracer techniques. *Geomicrobiol. J.* **1**, 11–28.
- Joye S. B., Connell T., Miller L. G., Oremland R. S., and Jellison R. (1999) Oxidation of ammonia and methane in an alkaline, saline lake. *Limnol. Oceanogr.* **44**, 178–188.
- Joye S. B., Orcutt B. N., Boetius A., Montoya J. P., Schulz H., Erickson M. J., and Lugo S. K. (2004) The anaerobic oxidation of methane and sulfate reduction in sediments from at Gulf of Mexico cold seeps. *Chem. Geol.* **205**, 3–4, 219–238.
- Joye S. B., MacDonald I. R., and Montoya J. P. (2005) Biogeochemical signatures of seafloor brines along the continental slope, Gulf of Mexico. *Biogeosciences* **2**, 637–671.
- Kalenetra K., Joye S. B., Sunseri N. R., and Nelson D. (2005) Novel, large vacuolate, nitrate-accumulating sulfur bacteria discovered in the Gulf of Mexico reproduce by reductive division in three dimensions. *Environ. Microbiol.* published online 15-June-2005 doi 10.1111/j.1452-2920.2005.00832.x.
- Katz M. E., Pak D. K., Dickens G. R., and Miller K. G. (1999) The source and fate of massive carbon input during the latest paleocene thermal maximum. *Science* **286**, 1531–1533.
- Kennicutt M. C., Brooks J. M., and Denoux G. J. (1988) Leakage of deep reserved petroleum to the near surface of the Gulf of Mexico continental slope. *Mar. Chem.* **24**, 39–59.
- Knittel K., Boetius A., Lemke A., Eilers H., Lochte K., Pfannkuche O., and Linke P. (2003) Activity, distribution and diversity of sulfate reducers and other bacteria in sediments above gas hydrate (Cascadia Margin, Oregon). *Geomicrobiol. J.* **20**, 269–294.
- Knittel K., Lösekann T., Boetius A., Kort R., and Amann R. (2005) Diversity and distribution of methanotrophic Archaea at cold seeps. *Appl. Environ. Microbiol.* **71**, 1, 467–479.
- Krüger M., Meyerdiecks A., Glockner F. O., Amann R., Widdel F., Kube M., Reinhardt R., Kahnt R., Bocher R., Thauer R. K., and Shima S. (2003) A conspicuous nickel protein in microbial mats that oxidize methane anaerobically. *Nature* **426**, 878–881.
- Krzycki J. A., Kenealy W. R., DeNiro M. J., and Zeikus J. G. (1987) Stable isotope fractionation by *Methanosarcina barkeri* during methanogenesis from acetate, methanol, or carbon dioxide-hydrogen. *Appl. Environ. Microbiol.* **53**, 2597–2599.
- Kvenvolden K. A. (1988) Methane hydrates and global change. *Global Biogeochem. Cycles* **2**, 3, 221–229.
- Kvenvolden K. A. (1993) Gas hydrates—Geological perspective and global change. *Rev. Geophys.* **31**, 173–187.
- Lanoil B. D., Sassen R., La Duc M. T., Sweet S. T., and Neelson K. H. (2001) Bacteria and Archaea physically associated with Gulf of Mexico gas hydrates. *Appl. Environ. Microbiol.* **67**, 11, 5143–5153.
- Linke P., Suess E., Torres M., Martens V., Rugh W. D., Ziebis W., and Kulm L. D. (1994) *In situ* measurements of fluid flow from cold seeps at active continental margins. *Deep-Sea Res.* **41**, 4, 721–739.
- Lovley D. R. and Klug D. D. (1986) Model for the distribution of sulfate reduction and methanogenesis in fresh-water sediment. *Geochim. Cosmochim. Acta* **50**, 1, 11–18.
- MacDonald I. R. (2002) *Stability and Change in Gulf of Mexico Chemosynthetic Communities. Volume II: Technical Report*. U.S. Department of the Interior, Minerals Management Service, Gulf of Mexico OCS Region.
- MacDonald I. R., Boland G. S., Baker J. S., Brooks J. M., Kennicutt M. C., and Bidigare R. R. (1989) Gulf of Mexico chemosynthetic communities II: Spatial distribution of seep organisms and hydrocarbons at Bush Hill. *Mar. Biol.* **101**, 235–247.
- MacDonald I. R., Guinasso N. L., Reilly J. F., Jr., Brooks J. M., Callender W. R., and Gabrielle S. G. (1990a) Gulf of Mexico hydrocarbon seep communities: VI. Patterns of community structure and habitat. *Geo-Mar. Lett.* **10**, 244–252.
- MacDonald I. R., Reilly J. F., Jr., Guinasso N. L., Brooks J. M., Carney R., Bryant W. A., and Bright T. (1990b) Chemosynthetic mussels at a brine-filled pockmark in the Northern Gulf of Mexico. *Science* **248**, 1096–1099.
- MacDonald I. R., Guinasso N. L., Sassen R., Brooks J. M., Lee L., and Scott K. T. (1994) Gas hydrate that breaches the sea-floor on the continental slope of the Gulf of Mexico. *Geology* **22**, 699–702.
- MacDonald I. R., Sager W. W., and Peccini M. B. (2003) Gas hydrate and chemosynthetic biota in mounded bathymetry at mid-slope hydrocarbon seeps: Northern Gulf of Mexico. *Mar. Geol.* **198**, 133–158.
- Manz W., Eisenbrecher M., Neu T. R., and Szewzyk U. (1998) Abundance and spatial organization of gram negative sulfate-reducing bacteria in activated sludge investigated by in situ probing with specific 16S rRNA targeted oligonucleotides. *FEMS Microbiol. Ecol.* **25**, 43–61.
- Michaelis W., Seifert R., Nauhaus K., Treude T., Thiel V., Blumenberg M., Knittel K., Gieseke A., Peterknecht F., Pape T., Boetius A., Amann R., Jørgensen B. B., Widdel F., Peckmann J., Pimenkov N., and Gulin M. B. (2002) Microbial reefs in the Black Sea fueled by anaerobic methane oxidation. *Science* **297**, 1013–1015.
- Milkov A. V. and Sassen R. (2000) Thickness of the gas hydrate stability zone, Gulf of Mexico continental slope. *Mar. Petrol. Geol.* **17**, 981–991.
- Mills H. J., Hodges C., Wilson K., MacDonald I. R., and Sobczyk P. A. (2003) Microbial diversity in sediments associated with surface-breaching gas hydrate mounds in the Gulf of Mexico. *FEMS Microbiol. Ecol.* **46**, 1, 39–52.
- Mills H. J., Martinez R. J., Story S., and Sobczyk P. A. (2004) Identification of members of the metabolically active microbial populations associated with *Beggiatoa* species mat communities from Gulf of Mexico cold-seep sediments. *Appl. Environ. Microbiol.* **70**, 9, 5447–5458.

- Nauhaus K., Boetius A., Krueger M., and Widdel F. (2002) *In vitro* demonstration of anaerobic oxidation of methane coupled to sulfate reduction from a marine gas hydrate area. *Environ. Microbiol.* **4**, 296–305.
- Orcutt B. N., Boetius A., Lugo S. K., MacDonald I. R., Samarkin V. A., and Joye S. B. (2004) Life at the edge of methane ice: Microbial cycling of carbon and sulfur in Gulf of Mexico gas hydrates. *Chem. Geol.* **205**, 3–4, 239–251.
- Oremland R. S. and Polcin S. (1982) Methanogenesis and sulfate reduction—Competitive and noncompetitive substrates in estuarine sediments. *Appl. Environ. Microbiol.* **44**, 6, 1270–1276.
- Orphan V. J., Hinrichs K.-U., Ussler W., III, Paull C. K., Taylor L. T., Sylva S. P., Hayes J. M., and Delong E. F. (2001a) Comparative analysis of methane-oxidizing archaea and sulfate-reducing bacteria in anoxic marine sediments. *Appl. Environ. Microbiol.* **67**, 4, 1922–1934.
- Orphan V. J., House C. H., Hinrichs K.-U., McKeegan K. D., and Delong E. F. (2001b) Methane-consuming archaea revealed by directly coupled isotopic and phylogenetic analysis. *Science* **293**, 484–487.
- Orphan V. J., House C. H., Hinrichs K.-U., McKeegan K. D., and Delong E. F. (2002) Multiple archaeal groups mediate methane oxidation in anoxic cold seep sediments. *Proc. Natl. Acad. Sci. U.S.A.* **99**, 7663–7668.
- Orphan V. J., Ussler W., III, Naehr T., House C. H., Hinrichs K.-U., and Paull C. K. (2004) Geological, geochemical and microbiological heterogeneity of the seafloor around methane vents in the Eel River Basin, offshore California. *Chem. Geol.* **204**, 265–289.
- Pancost R. D., Sinninghe Damste J. S., de Lint S., van der Maarel M. J. E. C., Gottschal J. C., and Party M. S. S. (2000) Biomarker evidence for widespread anaerobic methane oxidation in Mediterranean sediments by a consortium of methanogenic archaea and bacteria. *Appl. Environ. Microbiol.* **66**, 1126–1132.
- Pancost R. D., Bouloubassi I., Aloisi G., Sinninghe Damste J. S., and Party M. S. S. (2001) Three series of non-isoprenoidal dialkyl glycerol diethers in cold-seep carbonate crusts. *Org. Geochem.* **32**, 695–707.
- Paytan A., Mearon S., Cobb K., and Kastner M. (2002) Origin of marine barite deposits: Sr and S isotope characterization. *Geology* **30**, 747–750.
- Pernthaler A. and Amann R. (2004) Simultaneous fluorescence in situ hybridization of mRNA and rRNA in environmental bacteria. *Appl. Environ. Microbiol.* **70**, 9, 5426–5433.
- Pernthaler A., Pernthaler J., and Amann R. (2002) Fluorescence in situ hybridization and catalyzed reporter deposition for the identification of marine bacteria. *Appl. Environ. Microbiol.* **68**, 6, 3094–3101.
- Pimenov N., Savvichev A., Rusanov I., Egorov A. V., Gebruk A., Moskalev L., and Vogt P. R. (1999) Microbial processes of carbon cycle as the base of food chain of Haakon Mosby mud volcano benthic community. *Geo-Mar. Lett.* **19**, 1–2, 89–96.
- Reeburgh W. S. (1976) Methane consumption in Cariaco Trench waters and sediments. *Earth Planet. Sci. Lett.* **28**, 337–344.
- Sager W. W., MacDonald I. R., and Hou R. (2003) Geophysical signatures of mud mounds at hydrocarbon seeps on the Louisiana continental slope, northern Gulf of Mexico. *Mar. Geol.* **198**, 97–132.
- Sassen R. and MacDonald I. R. (1994) Evidence of structure H hydrate, Gulf of Mexico continental slope. *Org. Geochem.* **23**, 1029–1032.
- Sassen R., MacDonald I. R., Requejo A. G., Guinasso N. L., Kennicutt M. C., Sweet S. T., and Brooks J. M. (1994) Organic geochemistry of sediments from chemosynthetic communities, Gulf of Mexico slope. *Geo-Mar. Lett.* **14**, 110–119.
- Sassen R., Sweet S. T., DeFreitas A., Morelos J. A., and Milkov A. V. (2001) Gas hydrate and crude oil from the Mississippi Fan foldbelt, down-dip Gulf of Mexico Salt Basin: Significance to petroleum system. *Org. Geochem.* **32**, 999–1008.
- Sassen R., Roberts H. H., Carney R., Milkov A. V., DeFreitas A., Lanoil B. D., and Zhang C. L. (2004) Free hydrocarbon gas, gas hydrate and authigenic minerals in chemosynthetic communities of the northern Gulf of Mexico continental slope: Relation to microbial processes. *Chem. Geol.* **205**, 195–217.
- Schönhuber W., Fuchs B., Juretschko S., and Amann R. (1997) Improved sensitivity of whole-cell hybridization by the combination of horseradish peroxidase-labeled oligonucleotides and tyramide signal amplification. *Appl. Environ. Microbiol.* **63**, 8, 3268–3273.
- Sloan E. D. (1990) *Clathrate Hydrates of Natural Gases*. Marcel Dekker, New York.
- Sørensen K. B., Finster K., and Ramsing N. B. (2001) Thermodynamic and kinetic requirements in anaerobic methane oxidizing consortia exclude hydrogen, acetate and methanol as possible electron shuttles. *Microb. Ecol.* **42**, 1–10.
- Taylor J. and Parkes R. J. (1985) Identifying different populations of sulphate-reducing bacteria within marine sediment systems using fatty acid biomarkers. *J. Gen. Microbiol.* **131**, 631–642.
- Teske A., Hinrichs K.-U., Edgecomb V., de Vera Gomez A., Kysela D., Sylva S. P., Sogin M. L., and Jannasch H. W. (2002) Microbial diversity of hydrothermal sediments in the Guaymas Basin: Evidence for anaerobic methanotrophic communities. *Appl. Environ. Microbiol.* **68**, 4, 1994–2007.
- Thomas D. N., Zachos J. C., Bralower T. J., Thomas E., and Bohaty S. (2002) Warming the fuel for the fire: evidence for the thermal dissociation of methane hydrate during the Paleocene-Eocene thermal maximum. *Geology* **30**, 12, 1067–1070.
- Thomsen T. R., Finster K., and Ramsing N. B. (2001) Biogeochemical and molecular signatures of anaerobic methane oxidation in a marine sediment. *Appl. Environ. Microbiol.* **67**, 1646–1656.
- Torres M., McManus J., Hammond D. E., de Angelis M. A., Heeschen K., Colbert S. L., Tyron M. D., Brown K. M., and Suess E. (2002a) Fluid and chemical fluxes in and out of sediments hosting methane hydrate deposits on Hydrate Ridge, OR. I: Hydrological provinces. *Earth Planet. Sci. Lett.* **201**, 525–540.
- Torres M., McManus J., and Huh C.-A. (2002b) Fluid seepage along the San Clemente Fault scarp: Basin-wide compact on barium cycling. *Earth Planet. Sci. Lett.* **203**, 181–194.
- Torres M., Bohrmann G., Dubé T. E., and Poole F. G. (2003) Formation of modern and Paleozoic stratiform barite at cold methane seeps on continental margins. *Geology* **31**, 10, 897–900.
- Treude T. (2003) *Anaerobic Oxidation of Methane in Marine Sediments*. Ph.D. dissertation, University of Bremen.
- Treude T., Boetius A., Knittel K., Wallmann K., and Jørgensen B. B. (2003) Anaerobic oxidation of methane above gas hydrates at Hydrate Ridge, NE Pacific Ocean. *Mar. Ecol. Prog. Ser.* **264**, 1–14.
- Treude T., Krüger M., Boetius A., and Jørgensen B. B. (2005) Environmental control on anaerobic oxidation of methane in the gassy sediments of Eckernförde Bay (German Baltic). *Limnol. Oceanogr.* In press.
- Tyron M. D., Brown K. M., Torres M., Trehu A., McManus J., and Collier R. W. (1999) Measurements of transience and downward fluid flow near episodic methane gas vents, Hydrate Ridge, Cascadia. *Geology* **27**, 1075–1078.
- Valentine D. L. and Reeburgh W. S. (2000) New perspectives on anaerobic methane oxidation. *Environ. Microbiol.* **2**, 5, 477–484.
- Wallner G., Amann R., and Beisker W. (1993) Optimizing fluorescent in situ hybridization with rRNA-targeted oligonucleotide probes for flow cytometric identification of microorganisms. *Cytometry* **14**, 136–143.
- Weber A. and Jørgensen B. B. (2002) Bacterial sulfate reduction in hydrothermal sediments of the Guaymas Basin, Gulf of California, Mexico. *Deep-Sea Res. I* **49**, 827–841.
- Zehnder A. J. B. and Brock T. D. (1980) Anaerobic methane oxidation: Occurrence and ecology. *Appl. Environ. Microbiol.* **39**, 1, 194–204.
- Zhang C. L., Li Y., Wall J. D., Larsen L., Sassen R., Huang Y., Wang Y., Peacock A., White D. C., Horita J., and Cole D. R. (2002) Lipid and carbon isotopic evidence of methane-oxidizing and sulfate-reducing bacteria in association with gas hydrates from the Gulf of Mexico. *Geology* **30**, 3, 239–242.